DEVELOPMENT OF THREE-DIMENSIONAL MODELS FOR WOUND ROLLS

By

FENGZHU LI

Bachelor of Science

Nanjing Aeronautical Institute

Nanjing, China

1983

Submitted to the Faculty of the
Graduate College of the
Oklahoma State University
in partial fulfillment of
the requirements for
the Degree of
MASTER OF SCIENCE
December, 1994

DEVELOPMENT OF THREE-DIMENSIONAL

MODELS FOR WOUND ROLLS

Thesis Approved:

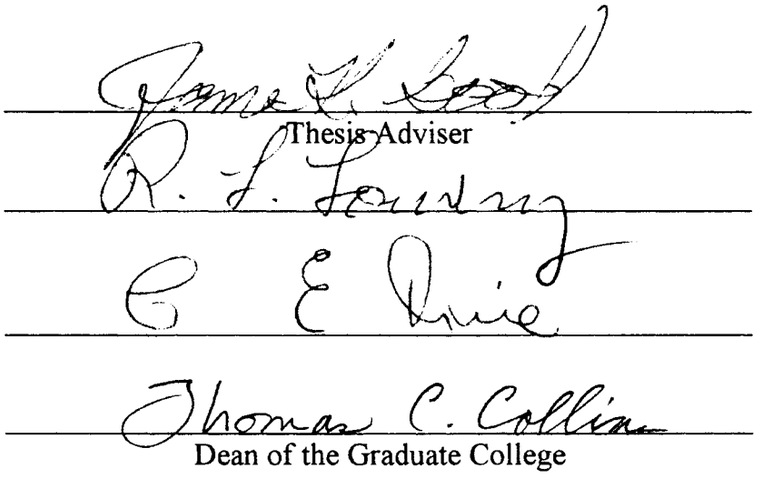

Thesis Adviser

Dean of the Graduate College

ACKNOWLEDGMENTS

I wish to express my sincere appreciation to my major advisor, Dr. J. Keith Good for his intelligent supervision, constructive guidance, and invaluable assistance. My sincere appreciation extends to my other committee members whose guidance, assistance, encouragement are also invaluable.

I greatly appreciated the school of Mechanical and Aerospace Engineering and the Web Handling Research Center for providing me with this research opportunity.

My fellow research assistants deserve a word of thanks for their friendship and for their part in making the Web Handling Research Center a pleasant place for work.

Finally, I would like to give my special gratitude and appreciation to my wife, Sun, for her love, and understanding throughout this two-year long process. Thanks also go to my parents, and my dear daughter, Yiyi, for their sacrifices.

TABLE OF CONTENTS

LIST OF TABLES

Table Page

LIST OF FIGURES

NOMENCLATURE

Cn	Coefficients of function of strain, n = 0, 1
C(j)	Core radius profile for segment j
E_t	Tangential Young's modulus of a wound roll
E_r	Radial Young's modulus of a wound roll
N(i , j)	Contact force applied on segment j, with i laps
R(i)	Characteristic radius (in.) for wound roll with i laps
Rmax(i)	The maximum radius of the wound roll profile with i laps
WOT(i , j)	Wound-On-Tension for segment j, lap i
T_s(i , j)	Predicted Web-Line-Tension for segment j with i laps
T_w(i , j)	Web-Line-Tension for segment j with i laps
M	Total numbers of segments
b	Width of the web
a(i , j)	Half width in Hertz theory of elastic contact
μ	Coefficient of friction
υ_{rt}, υ_{tr}	Poisson ratio.
ε_r(i , j)	Radial strain (in./in.)
ε_θ(i , j)	Circumferential strain(in./in.)
σ_r(i , j)	Radial stress
σ_θ(i , j)	Circumferential stress
Δ(i , j)	Gap between the winding web and wound roll

CHAPTER 1

INTRODUCTION

1.1 Scope and Literature Review

In many diverse and important industries, flexible sheet-like materials such as paper and film are temporarily stored in a continuous form by winding materials into rolls. These flexible and sheet-like materials are called webs. Over the past three decades, several papers have emerged in literature analyzing the stress distributions resulting from winding webs.

Wound roll models have primarily concentrated on the initial stresses developed in the winding process. The winding process is continuous, but it can be represented as a discrete addition of layers of finite thickness. Most winding models assume that a spiral of small thickness can be replaced by a ring of finite thickness [1, 5, 9]. As the layers are added, the stress state in the roll is altered and the radial stress accumulates continuously. The final stress state is the cumulative effect of all the wound layers. The quality of the final wound roll depends on the residual stresses in the roll during and after winding [1, 3, 4, 5]. A poor residual stress profile may deform the web to the point of permanent damage. Knowledge of the stresses within a wound roll has significant value.

The winding tension may be generated by providing torque to the core. This direct contact with the outer surface of the roll, which is called surface winding. In this study center winding will be considered.

An ideal web has uniform thickness in both the width and the length direction. The wound roll formed from ideal webs wound on a cylindrical core will form a perfect cylindrical roll as shown in Figure 1-1.

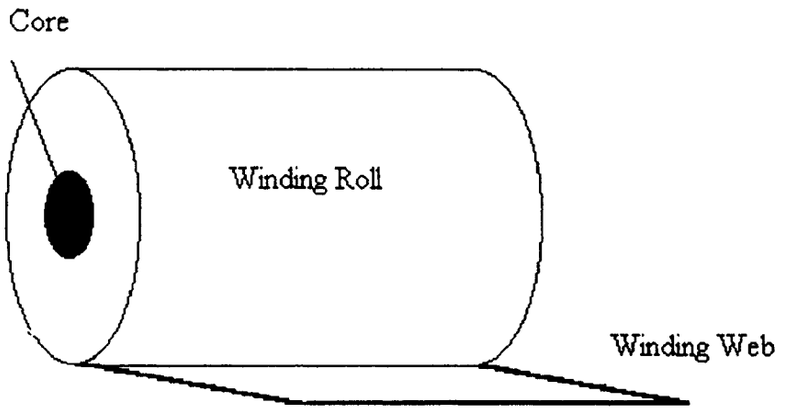

Figure 1-1. Ideal Web and Ideal Wound Roll

Based on this knowledge, several in-roll wound roll stress models have been described in literature [1, 5, 9, 10]. In these models, only stresses in the radial and circumferential directions have historically been taken into account. These models are two-dimension (2-D) models. Shown in Figure 1-2 are the significant elements on a center winding roll in analysis of 2-D wound roll models.

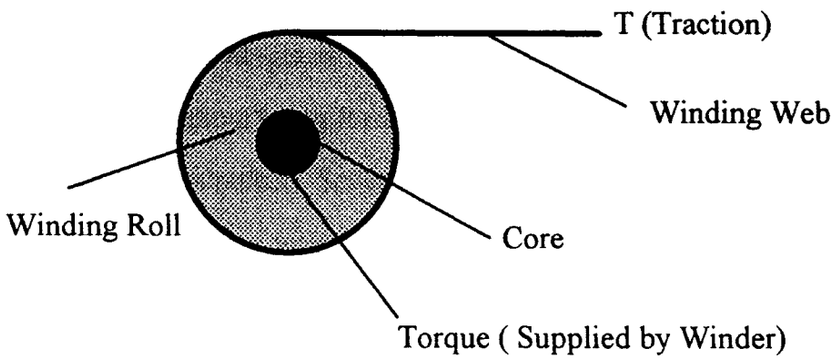

Figure 1-2. Two Dimensional Wound Roll Model

In the web handling industry, a common practice is to use a nip roller during winding. The nip roller is in contact with and applies a normal force to the winder roller. The web passes around the nip roller, through the contact zones between the nip roller and the winder roller, and onto the winder roller. A typical winding set up with nip roller is shown in Figure 1-3.

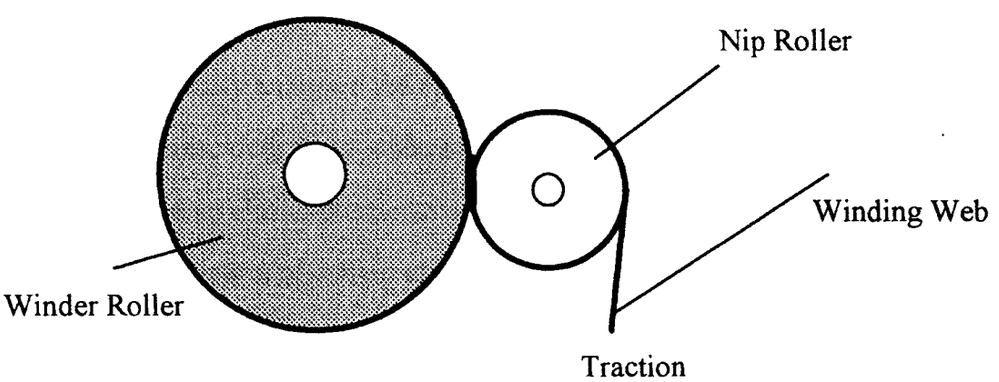

Figure 1-3. Winding Setup with Nip Roller

There are several advantages of winding with a nip roller, such as an increase in the wound in tension without being forced to increase web line tension and a reduction in the amount of air entrainment. Several studies concentrated on central winding with nip roller and surface winding with nip roller. Pfeiffer[11][12] performed the first work in nip mechanics in regarding winding. Good[4] and Cai[2] also worked on 2-D models related to nip mechanics. All of the 2-D models mentioned above take care of only ideal webs.

Real webs and real wound-rolls are more complicated than what the 2-D models describe. Real webs have thickness variations along widthwise and length directions which the 2-D model can not account for. In practical engineering, the width direction thickness variation in some webs, for example, webs produced on extrusion casting machines, tends to be persistent in the length direction. When webs with lengthwise persistent widthwise thickness variations are wound, the resulting wound rolls tend to have hardstreaks, or hard bands, which are areas of increased roll radius and increased interlayer pressures[6]. Hardstreaks often lead to local plastic deformation and may cause permanent distortion of the finished product due to extra high stress, stress relaxation and layer-to-layer adhesion.

Spitz[13] initially analyzed the effect of cross direction caliper variations in winding. In his research, Spitz made some assumptions about cross direction caliper distributions, and an elastic-plastic stress and strain curve. Through analysis, he concluded that variation of caliper along the widthwise direction will cause soft and hard spots on the final wound roll.

Hakiel[6] developed a 3-dimension (3-D) wound roll model which attempted to incorporate widthwise variation effects of caliper into a 2-D wound roll stress model. The 3-D model assumed the webs have lengthwise persistent widthwise thickness variations. The prediction of widthwise variations in the outside roll radius and winding tension are based on widthwise thickness variations of the web, mechanical

properties of the web, and the nominal value of winding tension. The model treated a 3-D wound roll as a combination of a series of 2-D segments which have different winding tensions of their own. The model employed the in-roll stress algorithm described by Hakiel[5] to compute the in-roll stress for the various widthwise segments of the roll. Although the model was shown to yield results which agreed with experiments for certain cases, there exists a great difference between the predicted and the experimental values. This difference is due to lack of coupling between outerlap analysis and in-roll displacement, especially for those kinds of webs where web compressibility is important.

Kedl[7] developed a 3-D wound roll model which considered widthwise effects with an emphasis on coupling in-roll displacements with the outerlap analysis. He first demonstrated that a 3-D wound roll can be treated as a combination of a series of deformation-independent segments and then computed the effects of cross web non-uniformity by dividing the wound roll into a series of 2-D segments. He assumed that all parts of the winding roll rotate at the same rate and the surface velocity at any position along the web width will be proportional to the increment radius times the roll rotational velocity. Through the continuity equation of the web, an estimation of the strain is obtained. Further, a compressibility correction is made to assure the validity of the model while layers increase. The lack of considering the in-roll dependence of stack modulus on load when calculating the in-roll displacement is the main drawback of this model.

Cole and Hakiel[3] developed a new 3-D wound roll model which is similar to Kedl's model[7]. The emphasis is placed on coupling between the outerlap analysis and the in-roll displacement. The major difference between the models of Cole and Hakiel, and Kedl are where the coupling occurs at each lap in the program while the roll is winding. This provides a way to retain the effect of the load-dependent stack modulus on in-roll displacements. In this newly developed model, an outerlap analysis based on

equilibrium considerations, which is the same as those used in Hakiel's model[6], is used to partition the winding tension for a particular lap. The widthwise distribution of the outside roll radius, the total winding tension in the lap, and the radial displacements in each segment due to addition of the current lap are used to calculate and update the outside roll radius, in-roll pressure and in-roll tension. This is the most recently developed 3-D model which accounts for thickness variation in the widthwise direction. Unfortunately, this model does not incorporate effects of nip rollers.

From the discussion above, it can be seen that, up to now, those most recent winding models are either 3-D models without considering the effects of the nip roller or 2-D models. As mentioned before, since winding with nip rollers is a common practice in the web handling industry, it is necessary to establish a 3-D wound roll model which considers not only widthwise thickness variation but also the effects of the nip rollers.

1.2 Objectives of Study

In the 2-D model, the wound-on-tension is a function of the nip load[2]:

$$WOT=T_w+\frac{\mu N}{h} \qquad (1\text{-}1)$$

where WOT is the web-on-tension, T_w is the web line tension and N is the normal contact force between the nip roller and the winding roll. This algorithm has been proven valid for a number of cases where the nip diameter is small enough(<20" diameter).

For wide rolls with caliper variation the nip load in (1-1) now varies across the width of the roll as the hardstreak contacts the nip roll prior to the rest of the wound

roll. Thus at a hardstreak the nip roll induces a greater wound-on-tension which results in yet a harder segment in the wound roll. In other words, since center winding web with non-uniform caliper results in a nonuniform wound-on-tension as shown by Hakiel, Cole and Hakiel, and Kedl[3,6,7], the effect of the nip roller compounds the wound-on-tension to even higher levels. Thus it is essential that 3-D wound roll models accurately predict the deformed radii of a winding roll (profiles of the roll) if an understanding of the effect of a nip on such rolls is to be developed.

In order to fully understand stress distributions and accurately predict the wound roll profile, a study of a 3-D wound roll with nip load is needed. The objectives of this research are:

1. to develop a working source code for Hakiel's 3-D uncoupled wound roll model.
2. to refine and develop a working source code for Cole and Hakiel's 3-D coupled wound roll model.
3. to develop a 3-D coupled wound roll model with nip roller and code it.

1.3 Arrangement of the Thesis

The preliminary study is discussed in Chapter 1, which includes the history review of 2-D and 3-D wound roll models. In Chapter 2, the 3-D working codes are developed based on the algorithms proposed by Hakiel[6], and Cole and Hakiel[3]. Applications of the 3-D wound roll models to wound rolls of web with sinusoidal thickness profiles are presented in Chapter 3. A 3-D wound roll model considering the nip roller is developed and presented in Chapter 4. In Chapter 5 conclusions and future work are included.

CHAPTER 2

DEVELOPMENT OF 3-D WOUND ROLL MODELS

As discussed in Chapter 1, 3-D wound roll models can successfully predict the in-roll stress distributions and wound roll radial profiles. These source codes are not public domain and were not available for this research. In this chapter, the required algorithms will be refined and working source codes of 3-D wound roll models will be developed.

2.1 Development of Hakiel's 3-D Uncoupled Wound Roll Model

Hakiel[6] once proposed a 3-D wound roll model which did not incorporate the displacement between outer lap and the wound roll beneath it. Since this model is simple, fast-running, and valid for incompressive materials, it is necessary to go over Hakiel's algorithm and develop an executable source code.

Consider a wound roll, which is composed of a series of 2-D segments, that has a roll profile r(i - 1 , j), and the winding web with thickness variation h(i , j). During winding of lap i under total web line tension T_a(i) onto that wound roll beneath the winding web, the lap i may or may not make contact with the wound roll beneath it. Since the web thickness has a variation in widthwise direction and the radius of wound roll for every segment also has a variation in widthwise direction, in those areas where contact is made, the lap being wound on will have the shape of the wound roll surface. The wound roll radius will be:

$$r(i,j) = r(i-1,j) + h(i,j) \qquad (2\text{-}1)$$

However, in those areas where no contact between winding web and the wound roll occurs, the web will be assumed to suspend as a straight cylindrical surface above the surface of the winding roll. The wound roll radius r(i , j) is not directly related to the previous roll radius of the wound roll, r(i - 1 , j), but related to some characteristic radius relevant to the whole wound roll. The winding process can be treated as the continuous addition of tensioned hoops. For each addition of a lap there must exist a relaxation radius which corresponds to an unstretched state of the hoop. This relaxation radius is the characteristic radius for the addition of web onto the wound roll. Let R(i) be the relaxation radius. Note that R(i) is a characteristic radius for the whole wound roll which has i laps , not a value of a specific segment. An approximation of the winding roll radius in the segments which have gapping occurring is:

$$r(i,j) = R(i) + h(i,j) \tag{2-2}$$

For segment j , the radial or circumferential tensional strain for lap i may be written as:

$$\varepsilon(i,j) = \frac{r(i,j) - R(i)}{R(i)} \tag{2-3}$$

If the web is unable to slide in the axial direction, the circumferential stress is then given by:

$$\sigma(i,j) = \frac{E_t}{1-\upsilon_t^2}\left(\frac{r(i,j) - R(i,j)}{R(i,j)}\right) \tag{2-4}$$

It should be pointed out that equations (2-3) and (2-4) are only applicable to segments where the winding web makes contact with the wound roll beneath it. In segments with no contact, gaps exist between the winding web and the wound roll. Those segments can not bear any force, and stress and strain there are assigned to:

$$\varepsilon\,(i,\,j) = 0 \tag{2-5}$$

$$\sigma(i,\,j) = 0 \tag{2-6}$$

By summing up the circumferential stress across the width of the web, the winding tension in the outer lap (the i^{th} lap) is predicted by:

$$T_a(i) = \sum_{1}^{M} \left\{ \sigma\,(i,j) \frac{bh}{M} \right\} \tag{2-7}$$

In order to maintain equilibrium in the outer lap of the winding roll, the predicted winding tension value must be equal to the wound-on-tension, which in centerwinding is assumed to be the web line tension T_w such that:

$$T_w(\,i\,) = T_a(\,i\,) \tag{2-8}$$

In solving equation (2-7) for the relaxation radius R(i), the secant method is used. After the relaxation radius R(i) is determined, equations (2-4), (2-6) are used to calculate the winding tension in each segment of the i^{th} layer. Then the in-roll pressure and in-roll tension are computed using the 2-D model proposed by Hakiel[5] due to the addition of the i^{th} layer.

In order to apply the above procedure to a wound roll with an unknown radius distribution, the initial roll radius profile before any lap is wound on is set to:

$$r(0, j) = c(j) \tag{2-9}$$

where c(j) is the core radius profile distribution.

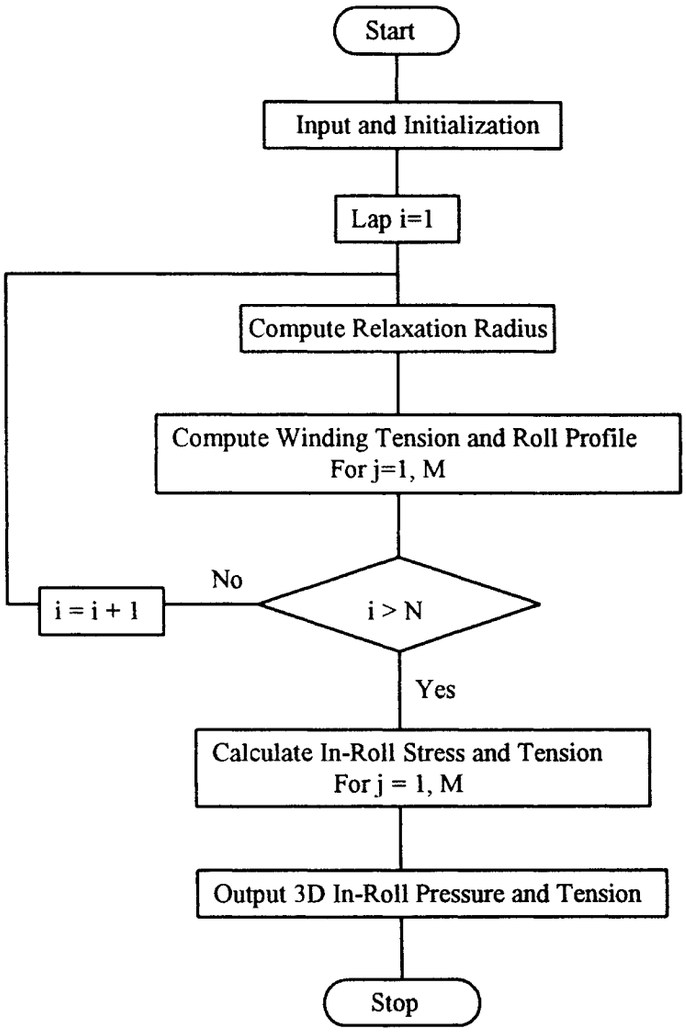

Figure 2-1. Flowchart of the Algorithm for Hakiel's 3-D Uncoupled Model

Through solving equation (2-7) and (2-8), R(1) is obtained and r(1 , j) is computed by using equation (2-1) or (2-2) when j is equal to 1. The above procedure is repeated for i = 2, 3, ... n, until all of the laps have been wound onto the roll. The flowchart of the algorithm for computing the roll profile, in-roll pressure, and in-roll tension is shown in Figure 2-1. The algorithm is coded in FORTRAN.

TABLE 2-1

PROPERTIES USED AS MODEL INPUTS

Core Diameter	5.0 inch
Wound Roll Diameter	15.0 inch
Average Web Thickness	0.004 inch
Young's Modulus	629, 200 psi
Stack Modulus	Exponential Function:
	$E_r(p) = C0 (1-e^{-p/c_1})$
	C0=361762.7 psi
	C_1=1254.2 psi
Poisson's Ratio υ_i	0.01
Core Modulus	512,500 psi
Winding Tension	2 lb/in
	or 4 lb/in (constant)

In order to verify the source code developed, program runs of simulations including two 10-inch-wide webs of 4-mil polymer film were wound on a core at two levels of winding tension: 2 lb/in and 4 lb/in. These rolls are the same as those used by Hakiel[6]. The web properties used as input are listed in TABLE 2-1. The 10 inch wide webs were divided into 20 one half inch wide segments and the thickness values for each segment are listed in TABLE 2-2.

TABLE 2-2

WEB THICKNESS VALUES OF SEGMENTS

Segment Number	Roll A (mils)	Roll B(mils)
1	3.934	3.958
2	3.932	3.971
3	3.927	3.967
4	3.942	3.969
5	3.956	3.970
6	3.964	3.975
7	3.962	3.983
8	3.953	3.984
9	3.947	3.978
10	3.942	3.985
11	3.939	4.007
12	3.939	4.010
13	3.936	4.010

TABLE 2-2 (continue)

14	3.919	4.011
15	3.912	4.012
16	3.912	4.011
17	3.898	3.999
18	3.886	3.990
19	3.882	3.990
20	3.900	3.993

Hakiel[[6] once constructed a core pressure measuring device to verify his theoretical 3-D wound roll model. This instrument used an LVDT sensor to traverse the width of the wound roll and determined the widthwise radius variations. In order to measure the in-roll stress a segmented core was constructed and instrumented with strain gages to permit interlayer pressure measurements to be made at the core at numerous widthwise locations. Since Hakiel's measurement is successful, his experimental results will be used as comparison basis in this study.

The values of in-roll pressure at the core are selected to verify the validity of the model. The outputs of core pressure from the execution of source code with comparison of the outputs provided by Hakiel are shown in Figure 2-2, Figure 2-3, Figure 2-4, and Figure 2-5, respectively. Note that in these figures "Measured" stands for experimental values obtained by Hakiel[6]; "Hakiel's" stands for predicted values provided by Hakiel[6]; and "Frank li's" stands for predicted values from the source code developed in this study.

From these figures it can be seen that the outputs from execution of the source code developed in this study and Hakiel's results are identical. This proved the validity of the source code developed in this study.

Comparing the measured values with predicted values, for some segments, the difference can be as high as 50%. This difference is due to a lack of coupling the displacements between the winding web and the wound roll, and this was the motivation to develop a more accurate model which is discussed in the next section.

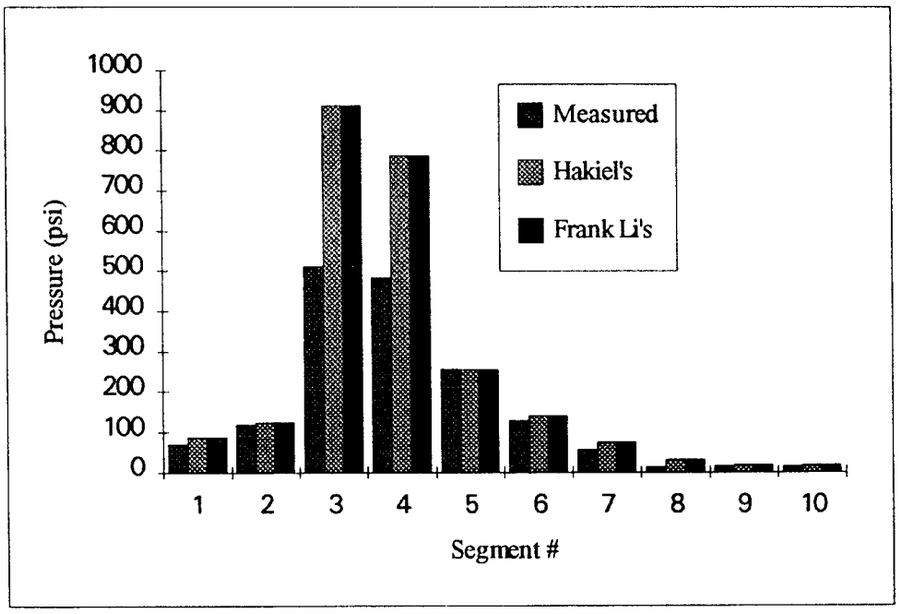

Figure 2-2. Comparison of Core Pressure for Roll A with Tension of 2 lb/in

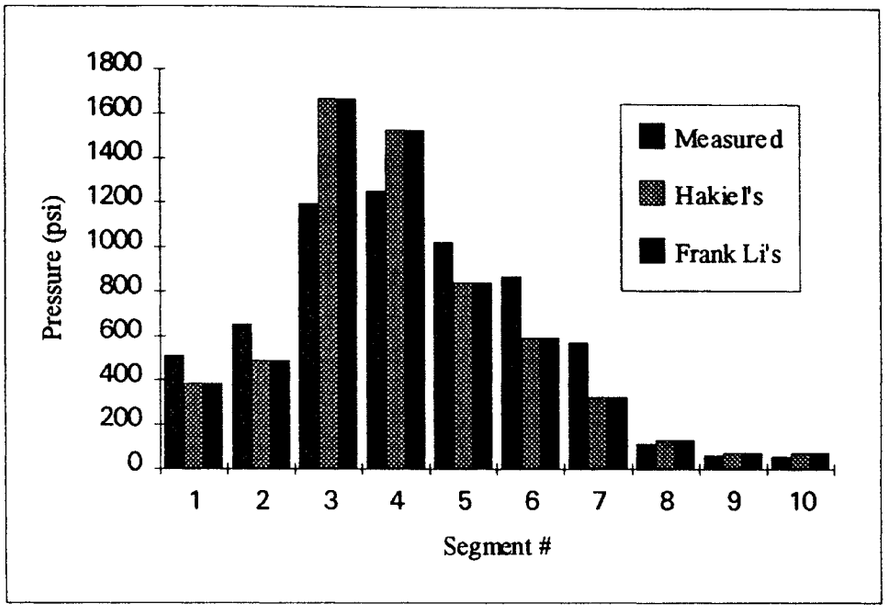

Figure 2-3. Comparison of Core Pressure for Roll A with Tension of 4 lb/in

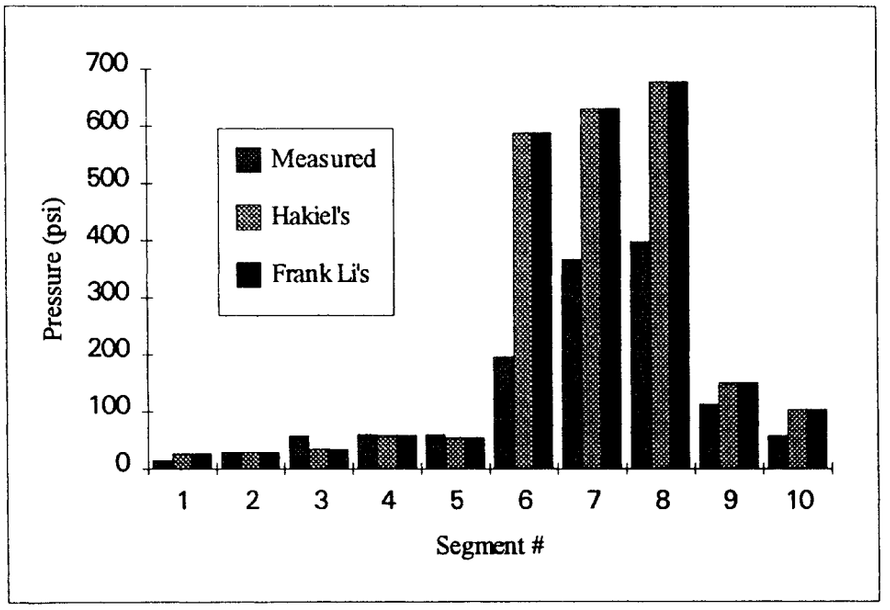

Figure 2-4. Comparison of Core Pressure for Roll B with Tension of 2 lb/in

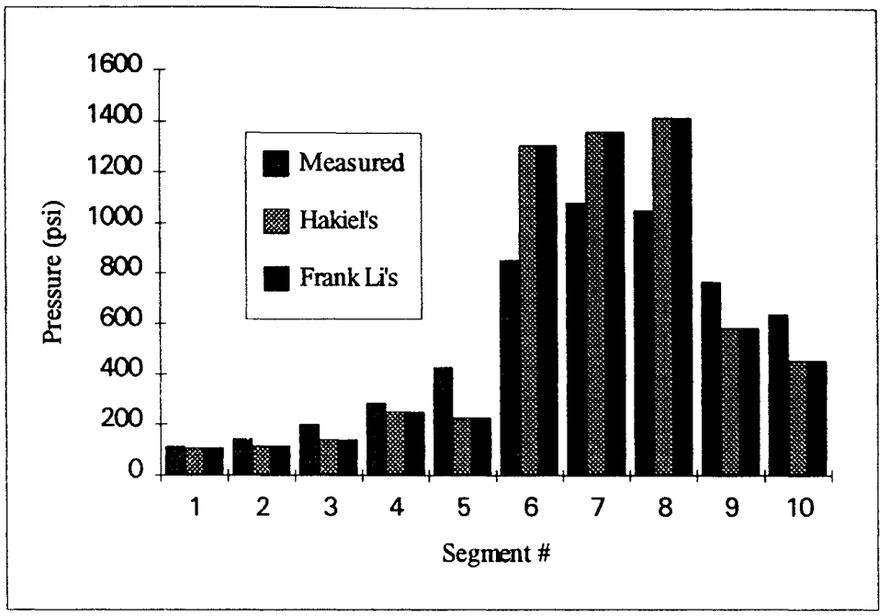

Figure 2-5. Comparison of Core Pressure for Roll B with Tension of 4 lb/in

2.2 Development of Cole and Hakiel's 3-D Coupled Wound Roll Model

As mentioned previously, 3-D models without coupled deformations can only be applicable to materials which are incompressible. For compressible materials, the impact of wound roll deformations in radial direction upon the segmented winding tensions should be considered[3].

Again, consider a wound roll, which is composed of a series of 2-D segments, that has a roll profile r(i -1, j). For every addition of a lap the relaxation radius R(i) is defined in the same way as those defined in Hakiel's 3-D uncoupled wound roll model. After an addition of the i^{th} lap subject to the web line tensions T_w(i -1, j), the winding web segments may or may not make contact with the wound roll beneath the web. For segments in which contact does occur, the wound roll profile will be:

$$r(i,j) = r(i-1,j) + u(i,j) + h(i,j) \qquad (2\text{-}10)$$

where u(i , j) is the radial displacement of the segment j due to addition of lap i and is defined positive radically outward. For segments where there is no contact, the roll profile will be given by:

$$r(i,j) = R(i) + h(i,j) \qquad (2\text{-}11)$$

The circumferential tensional strain and stress in the outer lap can be expressed using (2-3), (2-4), (2-5) and (2-6) as before.

Solving equation (2-10) is a somewhat difficult task because r(i , j) and u(i , j) are dependent on each other.

Because winding is regarded as a continuous process, the radial deformations due to two consecutive additions of layers to a wound roll should not vary dramatically. Thus the following assumption is made:

$$u(i,j) = u(i-1,j) + \Delta \qquad (2\text{-}12)$$

where Δ is a higher order term in regards to u(i , j). For simplicity, Δ can be ignored. So equation (2-12) becomes:

$$u(i,j) \approx u(i-1,j) \qquad (2\text{-}13)$$

Substitution of equation (2-13) into (2-10) yields:

$$r(i,j) = r(i-1,j) + u(i-1,j) + h(j) \qquad (2\text{-}14)$$

Equation (2-14) is a regressive formula, and the current radius can be calculated based on the previous radius profile and radial deformation.

Substitution of equation (2-14) into (2-4) yields:

$$\sigma(i, j) = \frac{E_t}{1-\upsilon_t^2}\left(\frac{r(i-1,j)+u(i-1,j)-R(i)}{R(i)}\right) \qquad (2\text{-}15)$$

Summing up all the circumferential stress across the width of the web, the predicted winding tension force in the outer lap is obtained by:

$$T_a(i) = \sum_{1}^{M}\left\{\sigma(i,j)\frac{bh}{M}\right\} \qquad (2\text{-}16)$$

In order to maintain equilibrium in the outer lap of the winding roll, the predicted winding tension value must be equal to the wound-on-tension, which in centerwinding is assumed to be the web line tension T_w such that:

$$T_w(i) = T_a(i) \qquad (2\text{-}17)$$

In order to use equation (2-14) to update the wound roll profile, the starting radius of the wound roll before any of the lap is wound onto the core is set to the radial profile of the core, that is:

$$r(0, j) = c(j) \qquad (2\text{-}18)$$

Although deformation of the core is allowed, for simplicity the initial displacement of the starting wound roll u(0, j) is set to:

$$u(0,j) = 0 \tag{2-19}$$

The subsequent displacement is calculated by:

$$u(i-1, j) = \varepsilon_\theta(i-1, j)\, r(i-1, j) \tag{2-20}$$

where $\varepsilon_\theta(i, j)$ is the circumferential strain due to an addition of the outer lap of the web, which is given by:

$$\varepsilon_\theta(i, j) = \sigma_\theta(i-1, j) - \upsilon_r \sigma_r(i-1, j) \tag{2-21}$$

where $\sigma_\theta(i, j)$, $\sigma_r(i-1, j)$ are in-roll stress in tangential and radial directions, respectively. The displacements described here are calculated using the Hakiel's algorithm[5].

The initial value of circumferential strain $\varepsilon_\theta(0, j)$ is assigned to:

$$\varepsilon_\theta(0, j) = 0 \tag{2-22}$$

Equations (2-14), (2-20) and (2-21) are used to update the wound roll profile during the addition of the i^{th} lap. $\sigma_\theta(i-1, j)$, $\sigma_r(i-1, j)$ and $u(i-1, j)$ are known variables which were calculated using Hakiel's algorithm[5] for the addition of the i-1 lap to the winding roll.

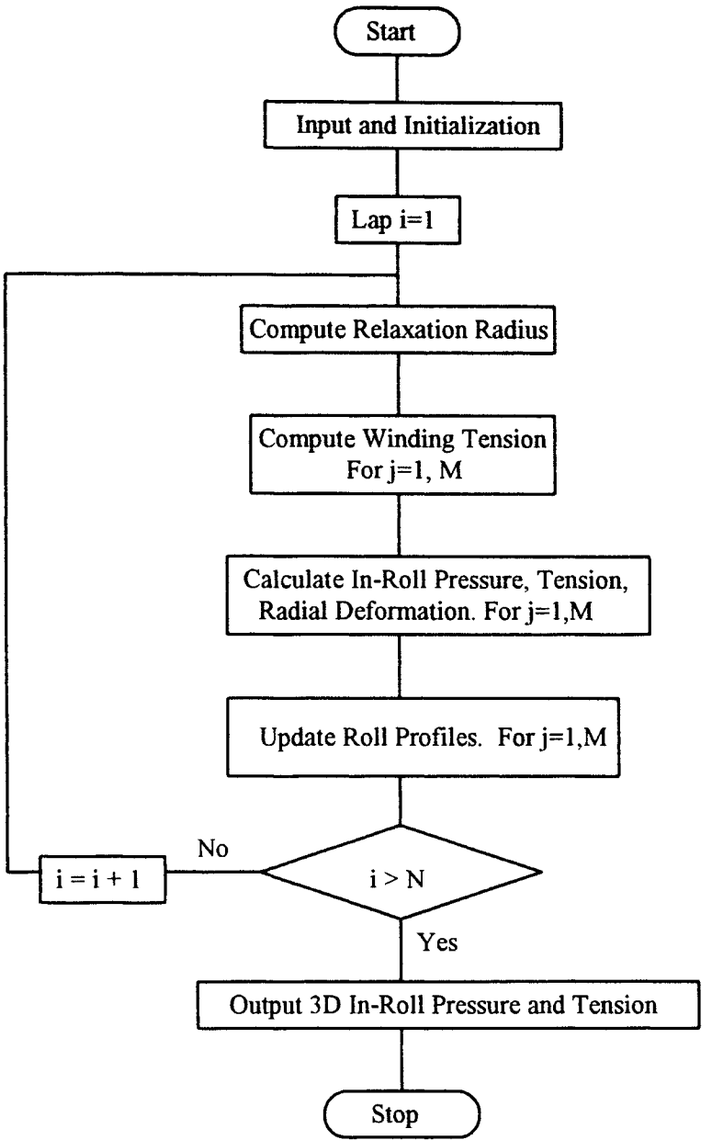

Figure 2-6. Flowchart of Cole and Hakiel's 3-D Coupled Model

The procedures described above are repeated for i=1, 2, ... n, until the whole roll is wound.

The flowchart of computational scheme described above is illustrated in Figure 2-6. The algorithms described above are coded in FORTRAN.

In order to verify the source code developed, program runs of simulations including two 10-inch-wide webs of 4-mil polymer film were wound on a core at two levels of winding tension: 2 lb/in and 4 lb/in. These rolls are the same as those used by Cole and Hakiel[2, 6]. The web properties used as input are listed in TABLE 2-1. The 10 inch wide webs were divided into 20 one half inch wide segments and the thickness values for each segment are listed in TABLE 2-2.

The values of in-roll pressure at the core are selected to verify the validity of the model. The outputs of core pressure from the execution of the source code with comparison of the outputs provided by Hakiel[6] and the outputs provided by Cole and Hakiel[3] are shown in Figure 2-7, Figure 2-8, Figure 2-9, and Figure 2-10, respectively. Note that in these figures "Measured" stands for experimental values obtained by Hakiel[6]; "Cole and Hakiel's" stands for predicted values provided by Cole and Hakiel[3]; "Frank Li's" stands for predicted values from the source code developed in this study.

From these comparison figures it can be seen that the source code developed in this study can predicate the in-roll stress quite well. For some low values the results from the source code developed in this study are better than Cole and Hakiel's results; for some larger values, however, differences are as high as 15 %. The difference between Frank Li's results and Cole and Hakiel's results might come from the usage of different algorithms in calculating displacements. For engineering purpose, this difference is allowable, and the validity of the source code has been demonstrated.

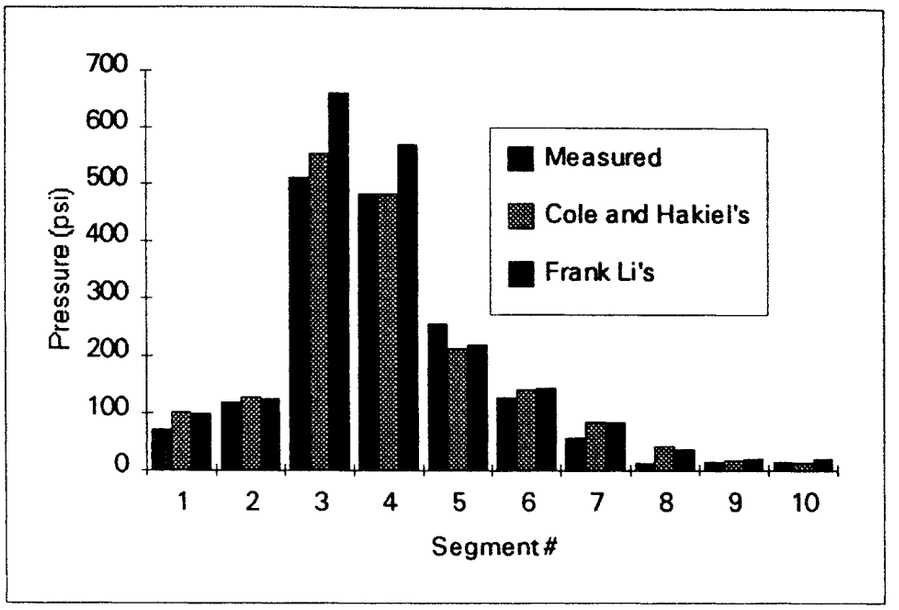

Figure 2-7. Comparison of Core Pressure for Roll A with Tension of 2 lb/in

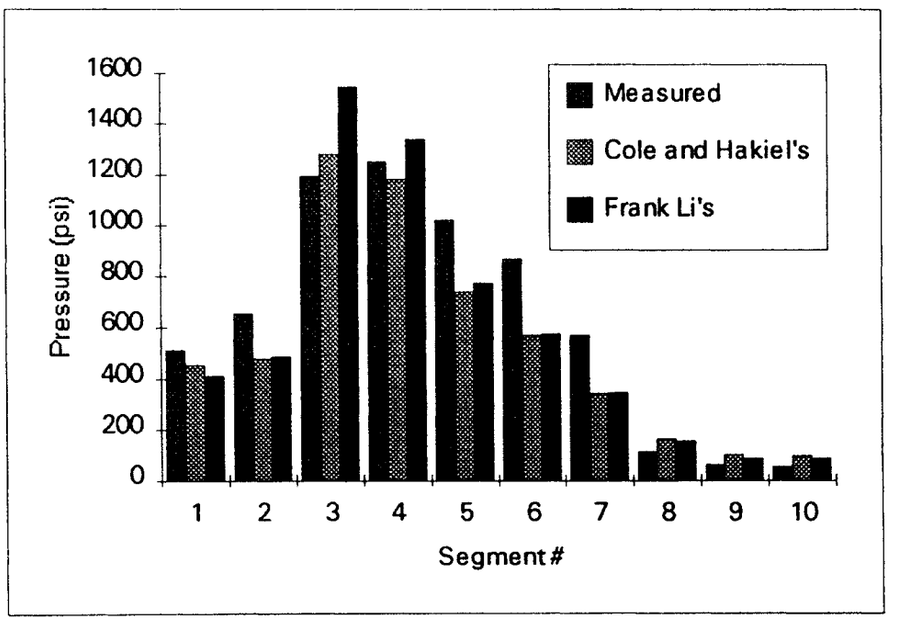

Figure 2-8. Comparison of Core Pressure for Roll A with Tension of 4 lb/in

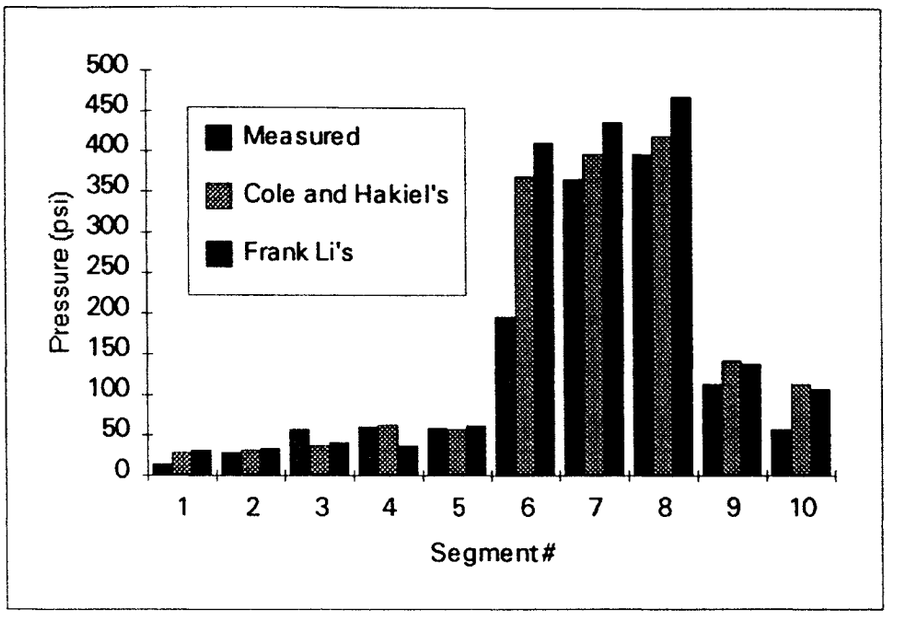

Figure 2-9. Comparison of Core Pressure for Roll B with Tension of 2 lb/in

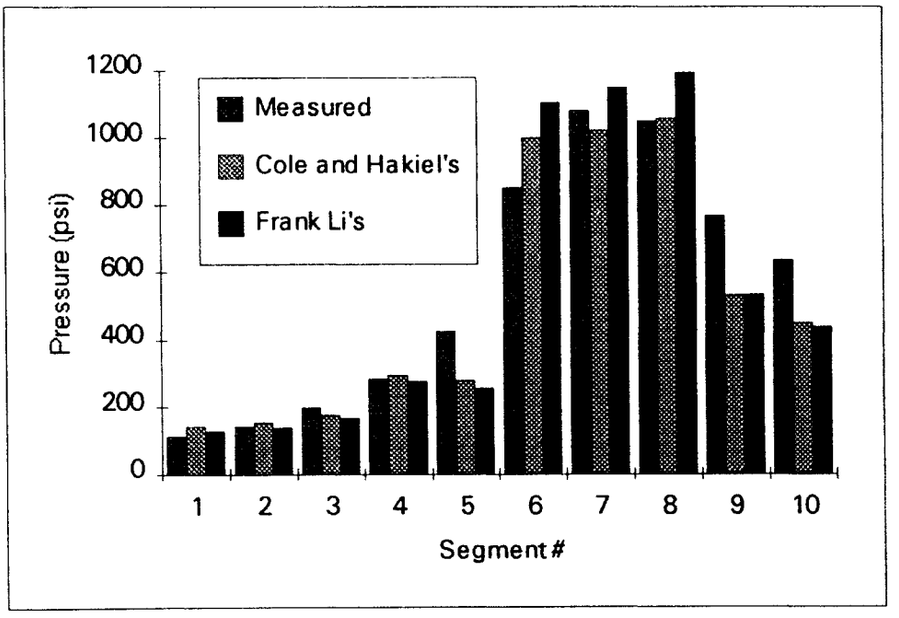

Figure 2-10. Comparison of Core Pressure for Roll B with Tension of 4 lb/in

CHAPTER 3

APPLICATIONS OF 3-D WOUND ROLL MODELS

Web thickness variations in widthwise direction are dependent on many factors. In the web handling industry, web thickness data are often obtained as the thickness is a measurement of quality. In Chapter 2, 3-D wound roll models and their source codes were developed and their validity has been proven. In this chapter, the 3-D models will be applied to wound rolls having artificial web thickness variation distribution in an effort to learn wound roll stresses.

3.1 Winding of Web with Sinusoidal Thickness Profile

In order to study the in-roll stress using the 3-D uncoupled and coupled wound roll models developed in Chapter 2, an arbitrary web thickness variation can be assumed for wound rolls. For simplicity, a web with sinusoidal thickness profile is used in this research.

Consider a wound roll which is composed of 21 segments. Suppose the winding web thickness variations in lengthwise direction are persistent and unchanged. But in widthwise direction, the thickness variation distribution of the web is in sinusoidal form. The properties used as model inputs are listed in TABLE 2-1 of Chapter 2, and the thickness variation parameters are listed in TABLE 3-1 and plotted in Figure 3-1. The nominal winding tension is kept constant, which is T_w = 4 lb/in.

TABLE 3-1

WEB THICKNESS VARIATION WITH SINE WAVE FORM

Number of Segment	Thickness (in.)
1	0.039849998
2	0.039933433
3	0.040008700
4	0.040068433
5	0.040106783
6	0.040119998
7	0.040106783
8	0.040068433
9	0.040008700
10	0.039933433
11	0.039849998
12	0.039766564
13	0.039691296
14	0.039631564
15	0.039593213
16	0.039579998
17	0.039593213
18	0.039631563
19	0.039691296
20	0.039766563
21	0.039849998

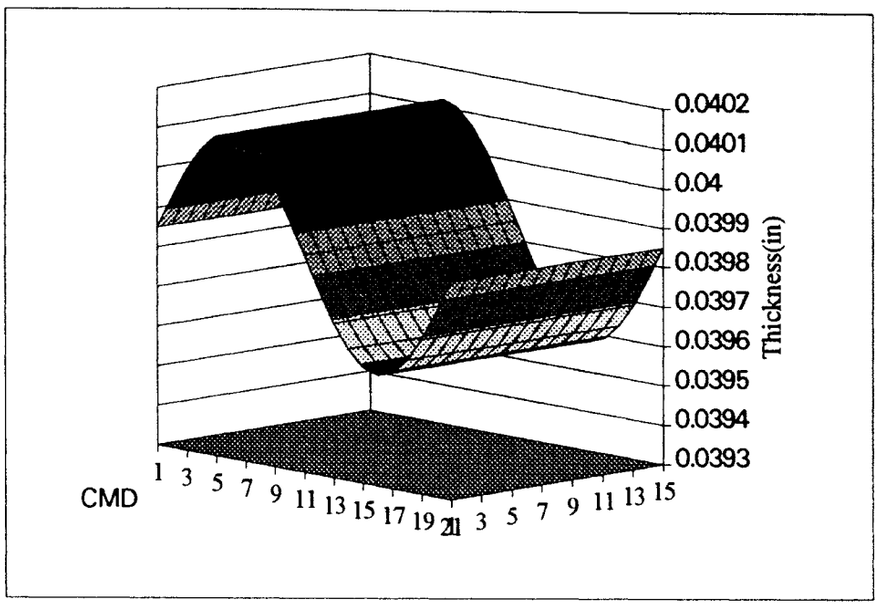

Figure 3-1. Sinusoidal Thickness Profile of Web

It is apparent that because of the thickness variations of the web in widthwise direction if too few segments are chosen to model the thickness variation that the output from the 3-D models will be less accurate. However, if too many segments are chosen, the computation will take more time. Thus computation time and computation accuracy are affected by the number of segments chosen to model the web thickness variation. For example, if web thickness is constant, it could be treated as a 2-D model and only one segment is required; if web thickness variations have a form of sinusoidal form in which the wave length is equal to the width of web, then more than two segments should be selected. In order to gain enough accuracy, 21 segments were used to calculate the in-roll stress in this application.

When using the 3-D wound model without coupling between displacements of winding web and wound roll beneath the web, the 3-D in-roll radial pressure distribution and 3-D in-roll tension distribution are shown in Figure 3-2, Figure 3-3, Figure 3-4, Figure 3-5, respectively.

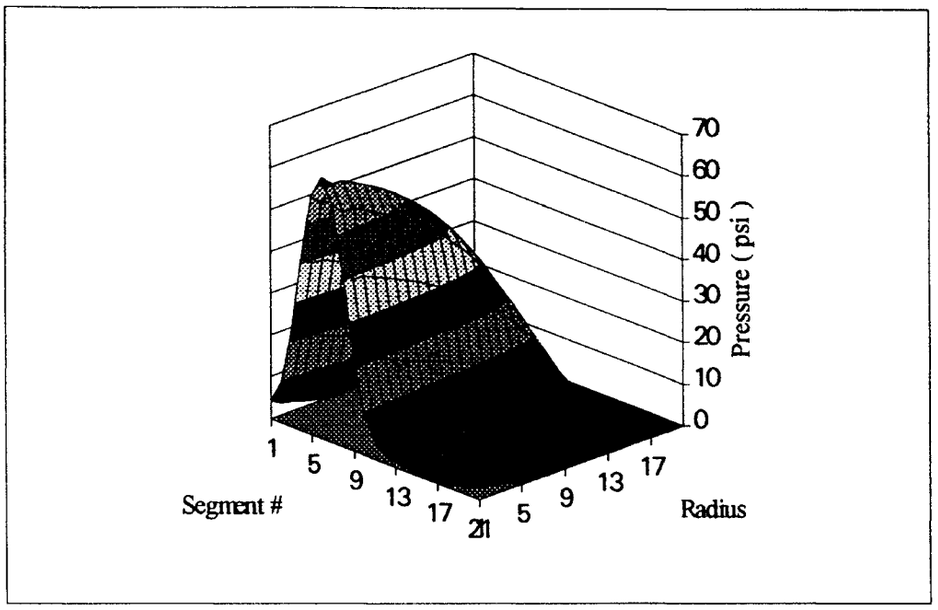

Figure 3-2. 3-D In-Roll Pressure Distribution for 21 Laps without Coupling

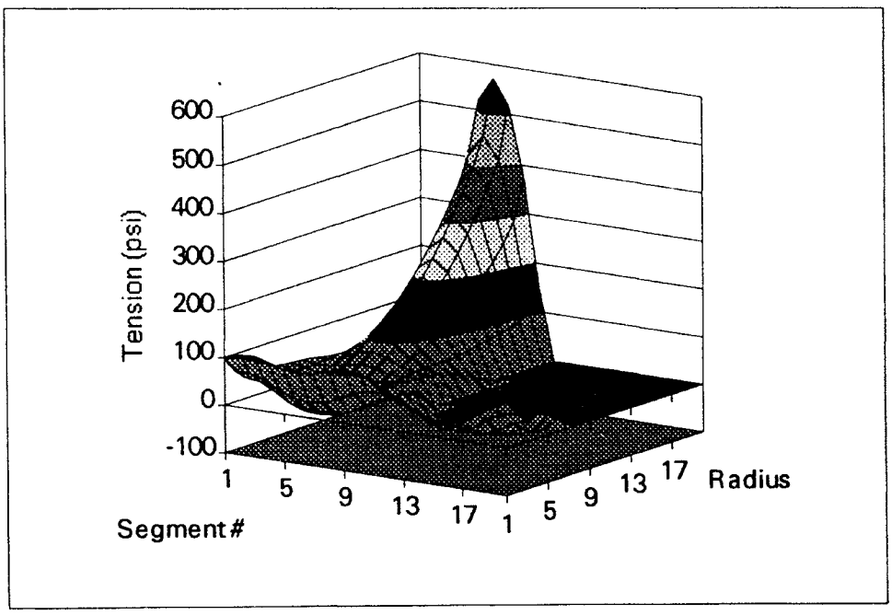

Figure 3-3. 3-D In-Roll Tension Distribution for 21 Laps without Coupling

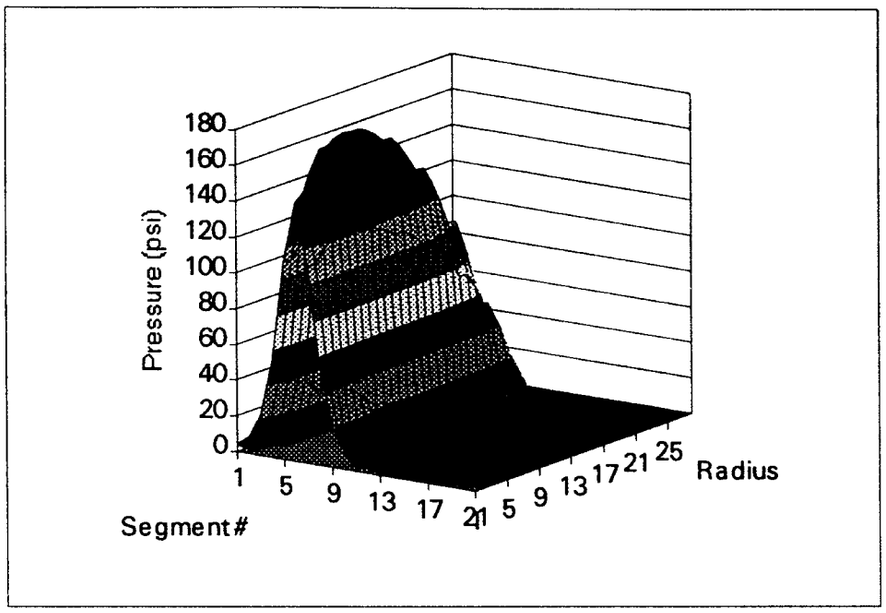

Figure 3-4. 3-D In-Roll Pressure Distribution for 241 Laps without Coupling

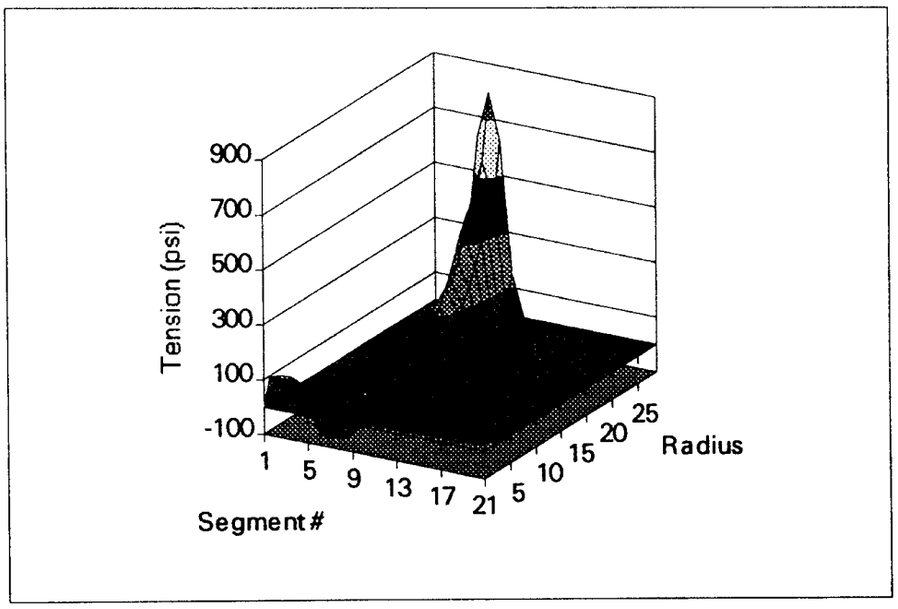

Figure 3-5. 3-D In-Roll Tension Distribution for 241 Laps without Coupling

Notice that in Figure 3-2 and Figure 3-3 the wound rolls have 21 laps of web, while in Figure 3-4 and Figure 3-5, the wound rolls have 241 laps of web. It is shown in these figures that the stress distribution in the widthwise direction may change

dramatically due to the web thickness variation. It is far from accurate if only average thickness is used as an input to compute the in-roll stress, that is to say, 2-D wound roll model should be replaced by 3-D wound roll model in order to accurately analyze the wound roll having web thickness variation. The in-roll radial pressure and in-roll tension are spatial surfaces since the winding web has thickness variation, and the maximum radial pressure corresponds to the location of maximum thickness of web. Comparison of Figure 3-2 with Figure 3-4 shows that with the increase of laps of wound roll, the shape of the in-roll pressure profile has changed greatly, and the maximum pressure is moved from near the core in Figure 3-2 to somewhere apart from the core in Figure 3-4. Although the number of laps is more than 10 times in Figure 3-4 than in Figure 3-2, the maximum in-roll pressure only increased by one time in Figure 3-4 than in Figure 3-2.

Using the same winding parameters for the 3-D wound roll model with coupled displacements, the 3-D in-roll radial pressure distribution and 3-D in-roll tension distribution are obtained and presented in Figure 3-6, Figure 3-7, Figure 3-8 and Figure 3-9, respectively.

From comparison of the outputs from the coupled model with the outputs from the uncoupled model which are shown in Figure 3-2, Figure 3-3, Figure 3-4 and Figure 3-5, it can be seen that all the results from the coupled model have lower values than those from the uncoupled model in the sense of absolute values. The impact of the coupled displacements is that the segmented tensions in the outer layer are distributed to more segments about the position where web thickness is greatest in contrast to the uncoupled model. It is interesting to compare the results in Figure 3-4 with those in Figure 3-8, and results in Figure 3-5 with those in Figure 3-9: because of the wound roll deformations, the maximum values of in-roll pressure in Figure 3-8 is only half of maximum values in Figure 3-4 and the maximum values of in-roll tension in Figure 3-9 is only one fourth of the maximum in Figure 3-5.

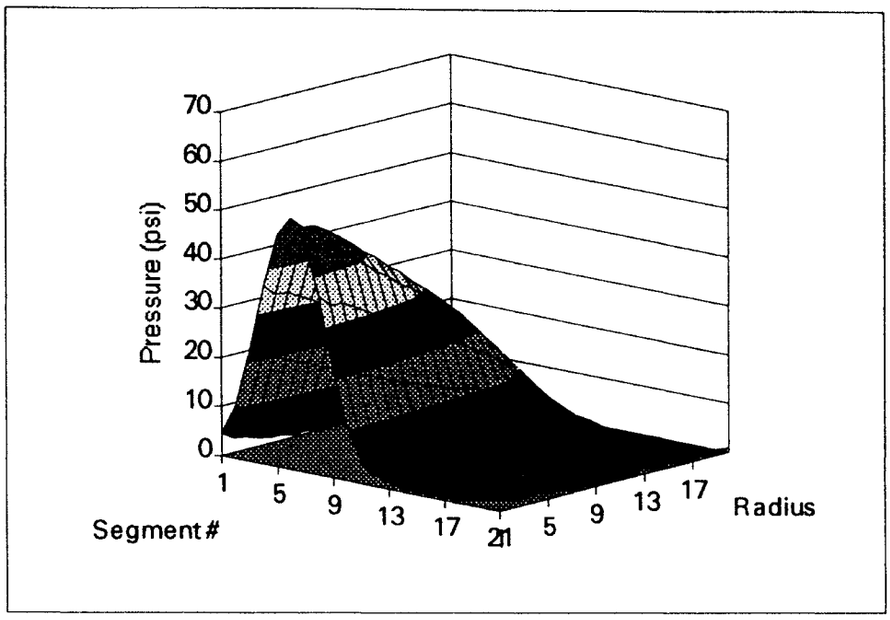

Figure 3-6. 3-D In-Roll Pressure Distribution for 21 Laps with Coupling

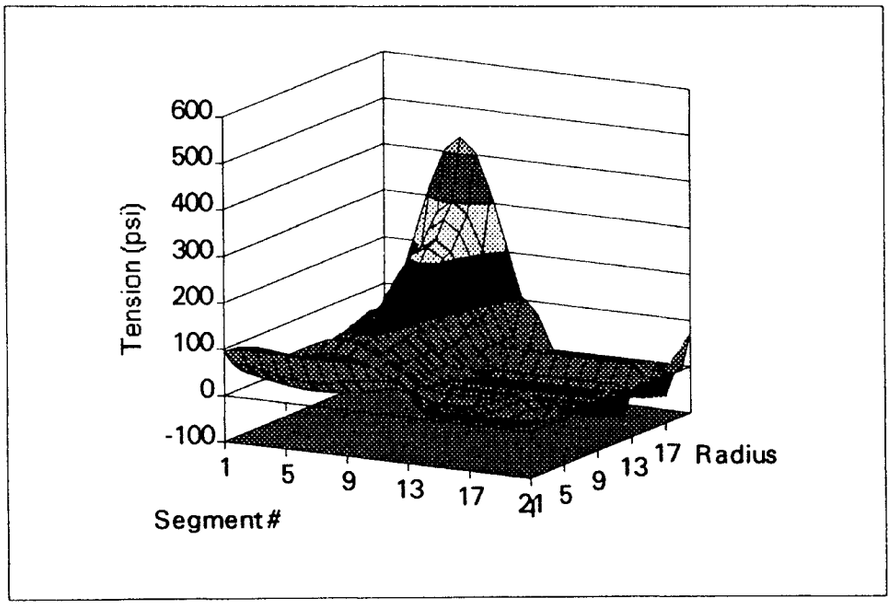

Figure 3-7. 3-D In-Roll Tension Distribution for 21 Lap with Coupling

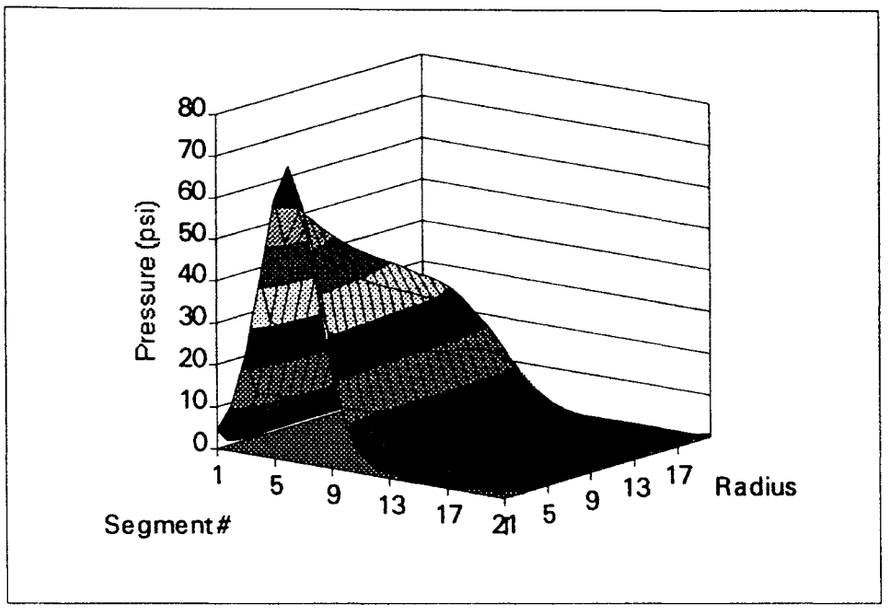

Figure 3-8. 3-D In-Roll Pressure Distribution for 241 Laps with Coupling

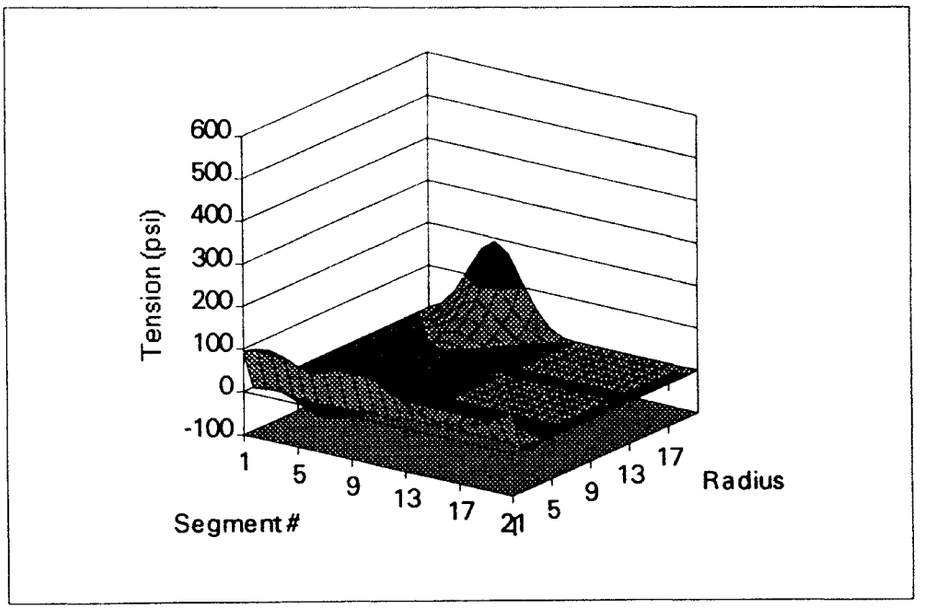

Figure 3-9. 3-D In-Roll Tension Distribution for 241 Laps with Coupling

CHAPTER 4

3-D WOUND ROLL COUPLED MODEL WITH NIP ROLLER

As discussed in previous chapters, winding with a nip roller is a common practice in engineering. Based upon the 3-D wound roll coupled model developed in Chapter 3, a 3-D wound roll coupled model with nip roller is developed in this chapter.

4.1 Modeling of 3-D Wound Roll Coupled Model with Nip Roller

Consider a winding roll which is being wound using a nip roller, and the roll has radius variations, as is shown in Figure 4-1. The radius variations may result from web thickness or core radius variations. Suppose the nip roller has a perfect cylindrical surface and has very high stiffness in radial direction. Because Young's modulus of the wound roll in radial direction is a function of in-roll pressure[13], and the in-roll pressure has a spatial distribution as shown in Chapter 3, when splitting the roll into segments, different segments will have different Young's modulus in radial direction.

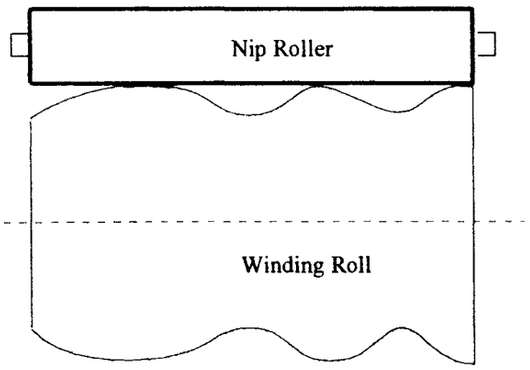

Figure 4-1. Exaggerated View of Winding Roll with Nip Roller

The winding process with a nip roller can be described as following: the wound roll with outside radius profile r(i , j) contacts the nip roller surface in some areas where the outside radii of the wound roll are greater than other areas. In the contact areas, the nip roller applies forces on the wound roll beneath the nip roller and results in local deformations in radial direction of the roll. Since the wound roll surface is uneven, when it is split into a series of segments, the applied force by the nip roller on each segment may be different, which depends on the radius and the Young' modulus of the segment. A model of the winding process is shown in Figure 4-2. Notice that an assumption that the nip roller remains parallel to the wound roll core, when force is applied, has been made.

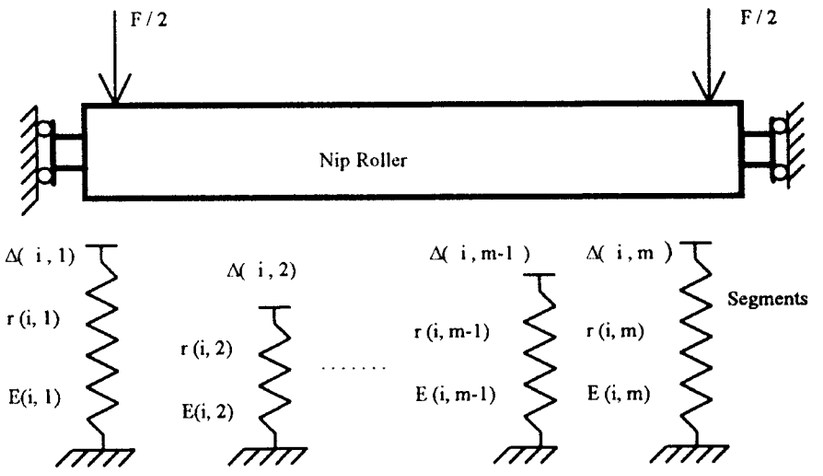

Figure 4-2. Model of Winding Roll with Nip Roller

For every addition of a lap, before a nip load is applied, the highest radius of all segments is named Rmax(i). The gaps between nip roller and the wound roll surface of segments are defined as:

$$\Delta(i , j) = Rmax(i) - r(i , j) \qquad (4\text{-}1)$$

After the nip load is applied, segments of the wound roll will be deformed in the radial direction according to the applied force on the segment and the average Young's modulus of that segment.

For segment j, the deformation is denoted by u(i , j). In order to simplify the algorithm, the radii of the segment are sorted in such an order as:

$$r(i , j-1) > r(i , j) \qquad \text{for } j = 2, \ldots, m \tag{4-2}$$

So:

$$r(i , 1) = Rmax(i) \tag{4-3}$$

and (4-1) yields:

$$\Delta(i , 1) = 0 \tag{4-4}$$

Gaps between the wound roll and the nip roller have such an order as:

$$\Delta(i , j-1) < \Delta(i , j) \qquad \text{for } j = 2, \ldots, m \tag{4-5}$$

When the nip roller contacts the wound roll, Hertz theory of elastic contact is assumed valid here[8]. The half width $a(i , j)$ is given by:

$$a^2(i, j) = \frac{4 N(i,j)\ r(i,j)}{\pi E} \tag{4-6}$$

and

$$\frac{1}{E} = \frac{1-\upsilon^2_{nip}}{E_{nip}} + \frac{1 - \upsilon^2_{rt}}{E_{wr}(i, j)} \tag{4-7}$$

where E_{nip} and $E_{wr}(i , j)$ are Young's modulus of the nip roller and the average Young's modulus, respectively, of segment j of a wound roll with i layers.

Since E_{nip} is about 10^6 psi , $E_{wr}(i , j)$ ranges from 25 to 2000 psi, and υ_{rt} is 0.01, the following approximation is valid:

$$E = E_{wr}(i, j) \tag{4-8}$$

The deformation of an isotropic roller due to cylindrical contact is given by[8]:

$$u(i, j) = \frac{N(i, j)(1 - \upsilon^2_n)}{\pi E_{wr}(i, j)} \left\{ 2 \ln\left(\frac{4\, r(i, j)}{a(i, j)}\right) - 1 \right\} \tag{4-9}$$

Due to the lack of a better algorithm, expression (4-9) will be used to determine the radial deformation u(i , j) of a nonlinear orthotropic wound roll due to nip impingement. Young's modulus of wound roll in radial direction, E_r,, is a function of in-roll pressure, p(i , j), where p(i , j) is a function of wound roll radius r(i , j). Hence, the Young's modulus of wound roll in radial direction can be expressed in a function of radius, that is, $E_r(r(i , j))$. The average Young's modulus of segment j of wound roll with i layers can be evaluated by:

$$E_{wr}(i , j) = \frac{1}{r(i, j) - r(0, j)} \int_{r(0,j)}^{r(i,j)} E_r(r(i, j))\, dr \tag{4-10}$$

When lap i is added to the winding roll which is composed of j segments with i-1 layers, contact conditions and applied forces for each segment are determined in the following algorithm:

First, assume only the segment with the highest radius(that is, segment 1, according to the sorting process previously describes) makes contact with the nip roller surface. The contact force is given by:

$$N(i , 1) = F \tag{4-11}$$

where F is applied force on the nip roller, which is in lb/in. The deformation in the contact segment will be given by:

$$u(i,1) = \frac{N(i,1)(1-\upsilon^2_{rr})}{\pi E_{wr}(i,1)}\left\{2\ln\left(\frac{4\,r(i,1)}{a(i,1)}\right) - 1\right\} \qquad (4\text{-}12)$$

where $a(i\ ,\ 1)$ is evaluated through (4-6).

u(i , 1) is evaluated using (4-12). If u(i , 1) < Δ(i , 2), the assumption that only segment 1 makes contact with the nip roller is confirmed, and the applied force on segment 1 and deformation are determined by (4-11) and (4-12), respectively. If u(i , 1) >Δ(i,2), go to the following step:

Assume both segment 1 and segment 2 make contact with the nip roller. The contact forces and the deformations are governed by the following equations:

$$u(i\ ,\ 1) = u(i\ ,\ 2) + \Delta(i\ ,\ 2) \qquad (4\text{-}13)$$

$$N(i\ ,\ 1) + N(i\ ,\ 2) = F \qquad (4\text{-}14)$$

where u(i , 1) and u(i , 2) can be substituted by right side of equation (4-9) when j is substituted by 1 and 2.

Through solving (4-13) and (4-14) simultaneously, u(i , 1) and N(i , 1) are updated and u(i , 2) and N(i , 2) are obtained. If u(i , 1) < Δ(i , 3), the assumption that only the segment 1 and segment 2 make contact with nip roller are confirmed, and the contact forces and the deformation are given through solving equation (4-13) and (4-14), simultaneously. If u(i , 1) > Δ(i , 3), go to the following step:

Assume segment 1, segment 2 and segment 3 make contact with the nip roller at the same time. The deformation and contact forces are governed by the following equations:

$$u(i,1) = u(i,2) + \Delta(i,2) \quad (4\text{-}15)$$

$$u(i,1) = u(i,3) + \Delta(i,3) \quad (4\text{-}16)$$

$$N(i,1)+N(i,2)+N(i,3) = F \quad (4\text{-}17)$$

where u(i , 1), u(i , 2) and u(i , 3) can be substituted by the right side of equation (4-9) when j is substituted by 1, 2 and 3. After substitution of u(i , 1), u(i , 2) and u(i , 3), (4-15) and (4-16) become two equations with unknown N(i , 1), N(i , 2) and N(i , 3). Through solving the three equations (4-15), (4-16) and (4-17) for three unknowns N(i , 1), N(i , 2) and N(i , 3) simultaneously, N(i , 1), N(i , 2) and N(i, , 3) are obtained. Hence, u(i , 1), u(i , 2) and u(i , 3) are obtained through (4-12). If $u(i,1) < \Delta(i,4)$, the assumption that segment 1, segment 2 and segment 3 are the only contacting segments are confirmed. If $u(i,1) > \Delta(i,4)$, go to the following step:

.....

The procedures described above are repeated until contact conditions and the applied forces are determined for lap i.

After the contact condition and the applied forces are determined for lap i, the web-on-tension for segment j are calculated by[4]:

$$WOT(i,j) = T_w(i,j) + \frac{\mu N(i,j)}{h(i,j)} \quad (4\text{-}18)$$

Where $T_w(i,j)$ is calculated in Chapter 2.

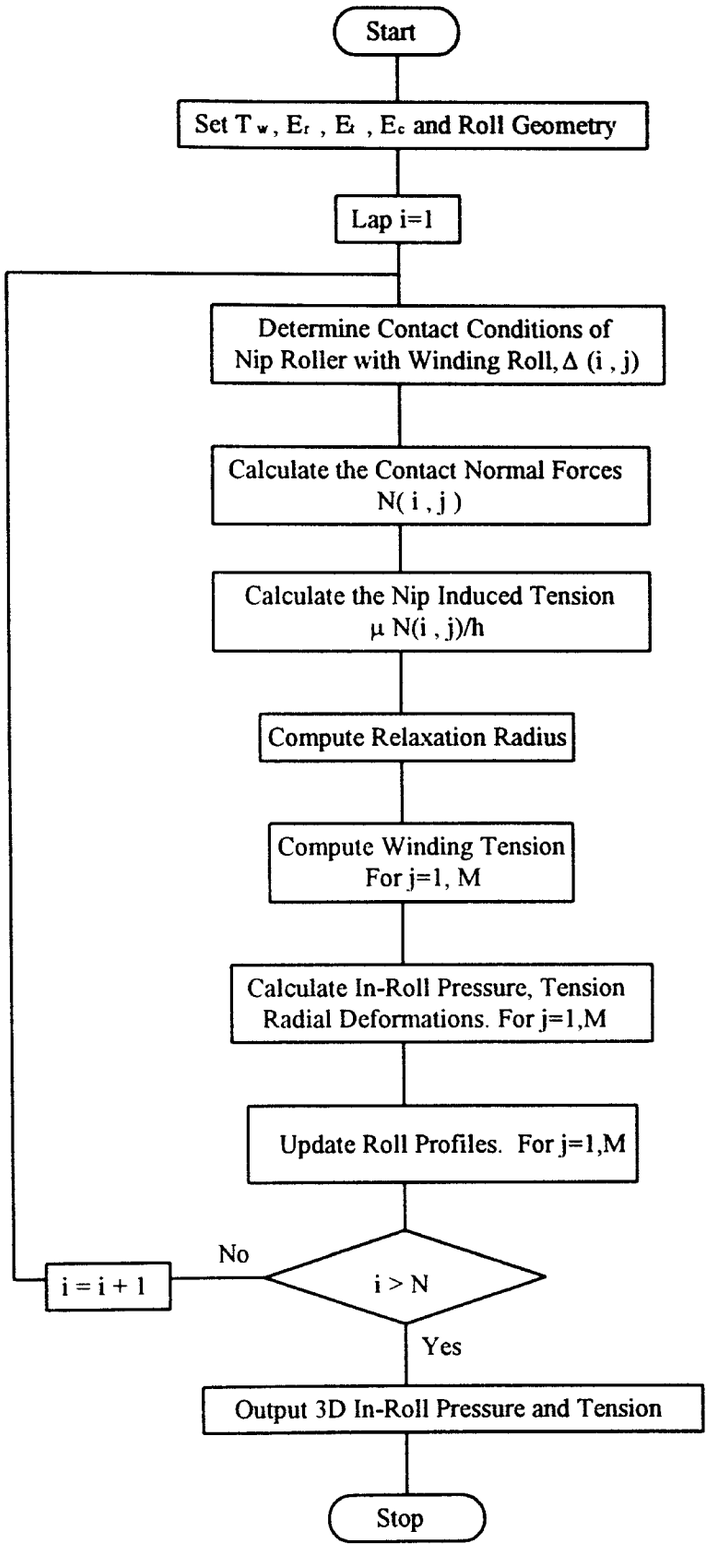

Figure 4-3. Flowchart of 3-D Wound Roll Coupled Model with Nip Roller

WOT(i , j) is substituted into the 3-D wound roll coupled model developed in Chapter 3 to calculate the in-roll pressure and wound roll profile until the whole roll is wound. The flowchart for the algorithm is shown in Figure 4-3.

4.2 Computations and Comparisons

Two wound rolls with two levels of nip forces are processed using the 3-D wound roll coupled model with nip roller in this section. As comparison, the same wound rolls are processed using 3-D wound roll coupled model. The input parameters are listed in TABLE 2-1 of Chapter 2, and they are the same input parameters as Cole and Hakiel used in their cases[3]. For simplicity, the wound rolls are only composed of 2 segments with 300 layers and the web line tensions are kept constant and equal to 7 N/cm. The web thickness variations in the widthwise direction are listed in TABLE 4-1. Notice that data in Set A are the maximum and minimum web thickness variation used in Cole and Hakiel's cases, while data in Set B are the two closest values.

TABLE 4-1

WEB THICKNESS VARIATION

	Set A	Set B
Segment 1	0.01007625 cm	0.01010202 cm
Segment 2	0.01019033 cm	0.01011202 cm

Figure 4-4 to Figure 4-7 display computational results from use of the 3-D wound roll coupled model. Since the web thickness variation in Set A is greater than that in set B, the height of hardstreak of the wound roll for Set A is greater than that for Set B, as is shown in Figure 4-4, and figure 4-5. The in-roll pressure for the case in Set B is much more even than that for the case in Set A, as is shown in Figure 4-6, and Figure 4-7.

This is because the wound roll of case in Set B had a lower height of the hardstreak and the web line tension could be distributed more evenly in Set B than in Set A.

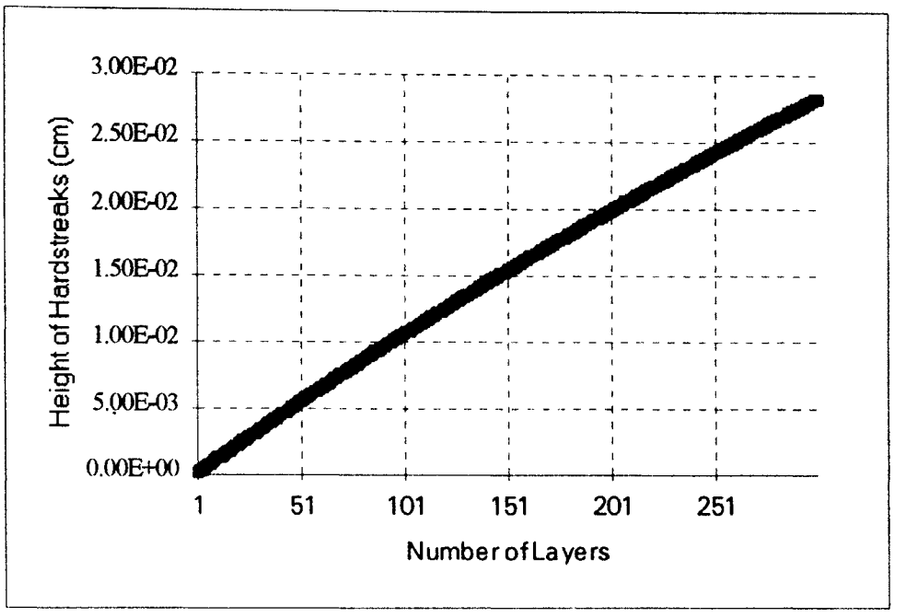

Figure 4-4. Height of Hardstreak for Set A without Nip Roller

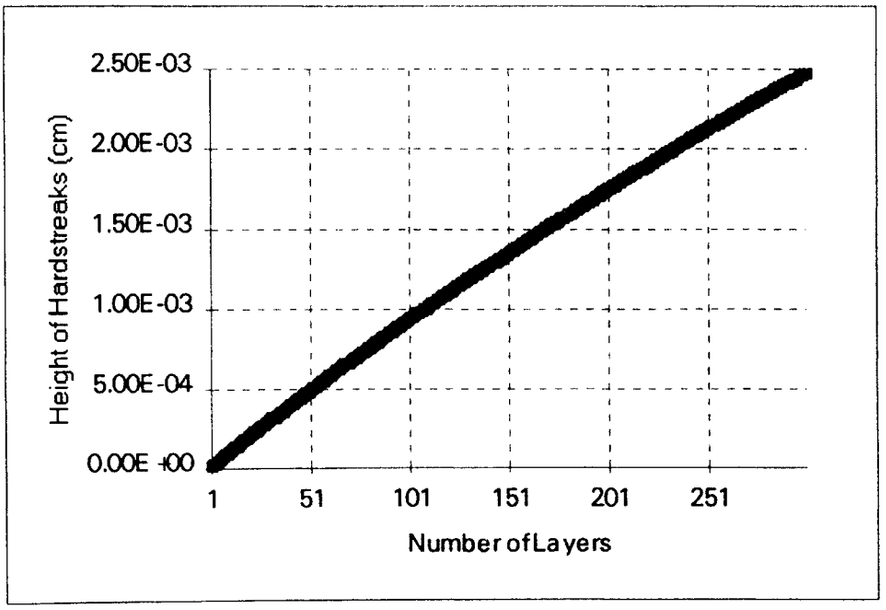

Figure 4-5. Height of Hardstreak for Set B without Nip Roller

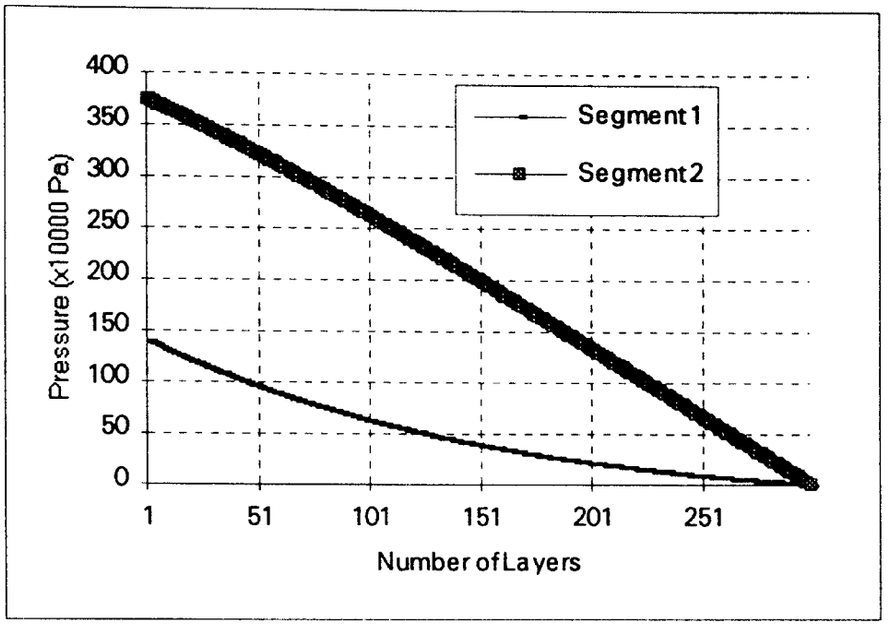

Figure 4-6. In-Roll Pressure for Set A without Nip Roller

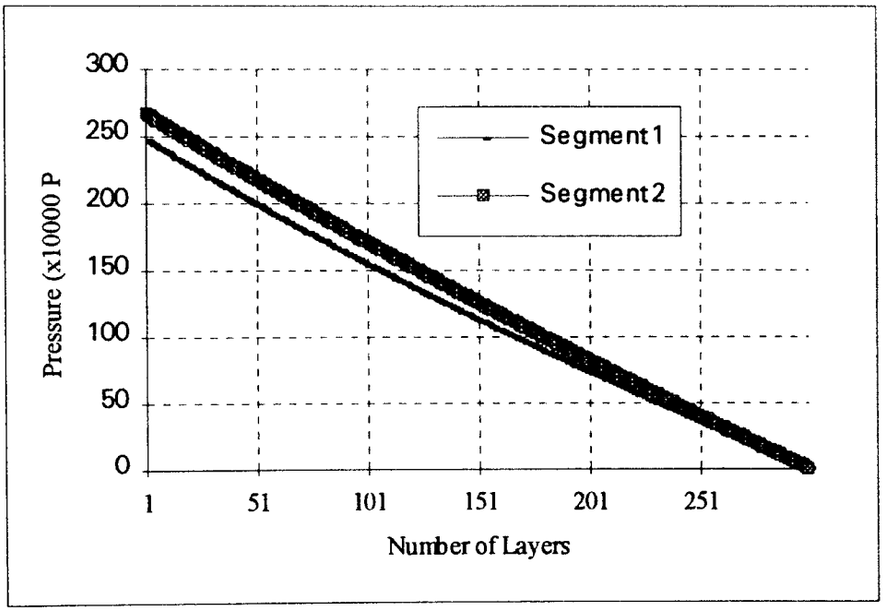

Figure 4-7. In-Roll Pressure for Set B without Nip Roller

Figure 4-8 to Figure 4-19 are computational results using the 3-D wound roll coupled model with nip roller. Notice that the nip roller is not applied until 10 layers of web are accumulated.

The applied forces on the two segments due to application of the nip roller are plotted in Figure 4-8 to Figure 4-11. From these figures it can be seen that in the cases shown in Figure 4-8, Figure 4-9 and Figure 4-10, only segment 2 carries the nip force, which indicates that only segment 2 makes contact with the nip roller. In the case shown in Figure 4-11, two segments make contact with the nip roller only at the beginning of stage of application of the nip roller. With continuous addition of laps, the contact condition changes to the case in which only one segment remains contacting.

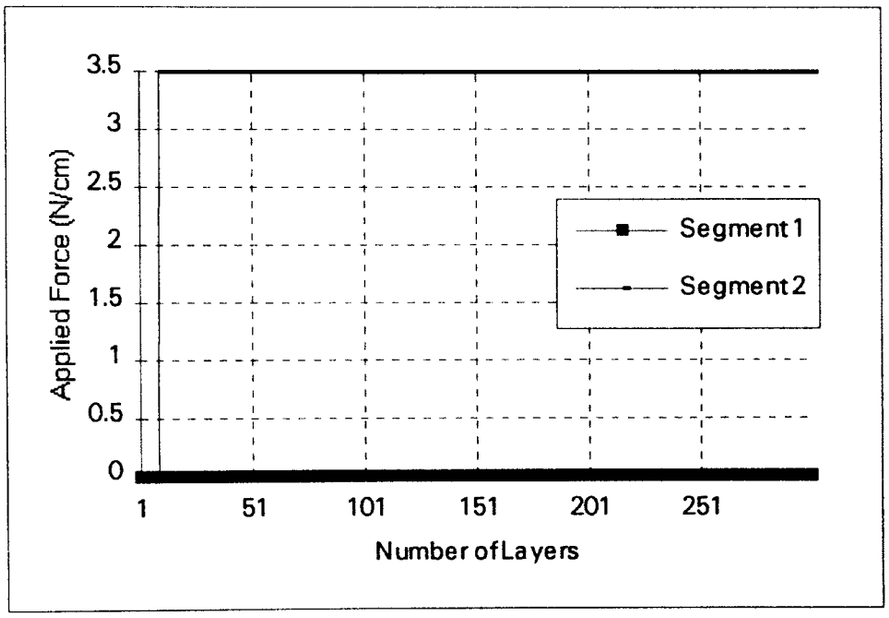

Figure 4-8. Applied Force Distribution for Set A with Nip Force 3.5 N/cm

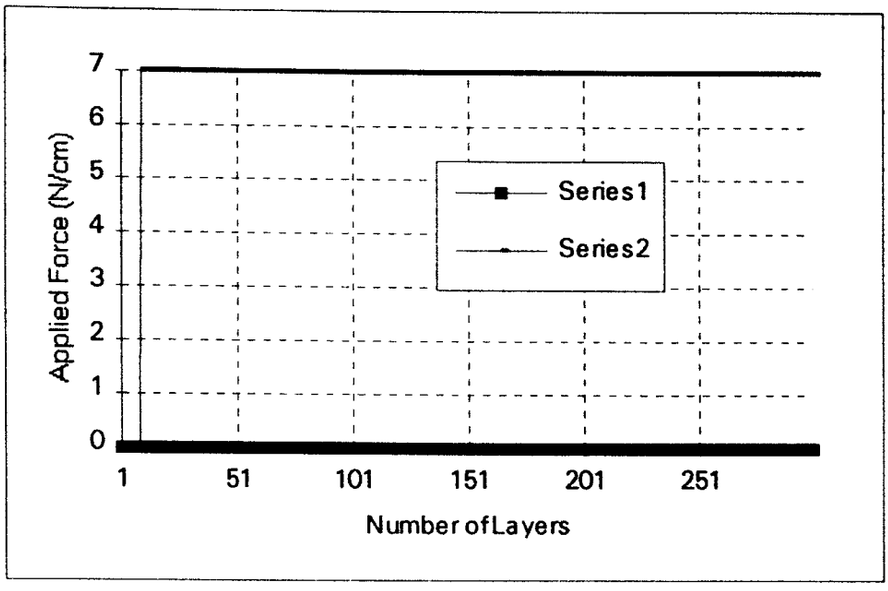

Figure 4-9. Applied Force Distribution for Set A with Nip Force 7 N/cm

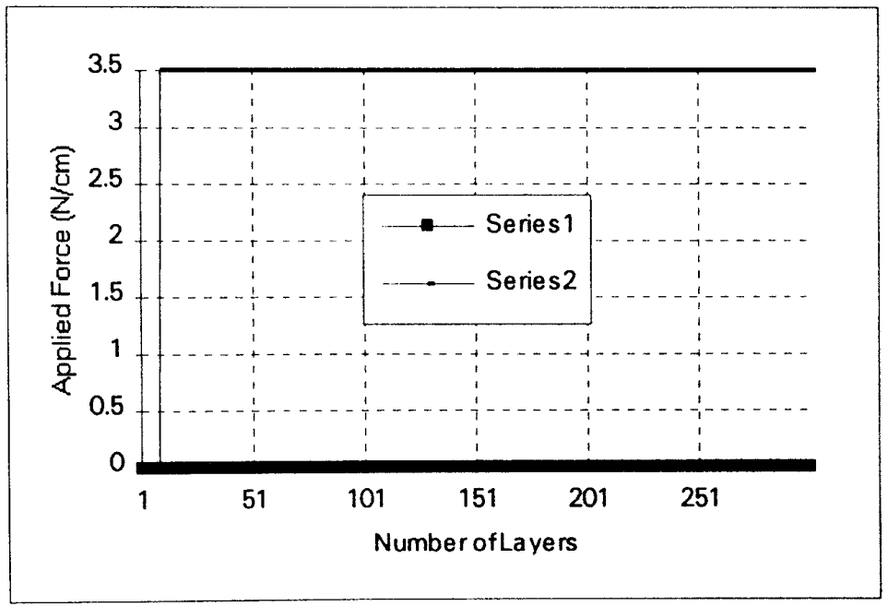

Figure 4-10. Applied Force Distribution for Set B with Nip Force 3.5 N/cm

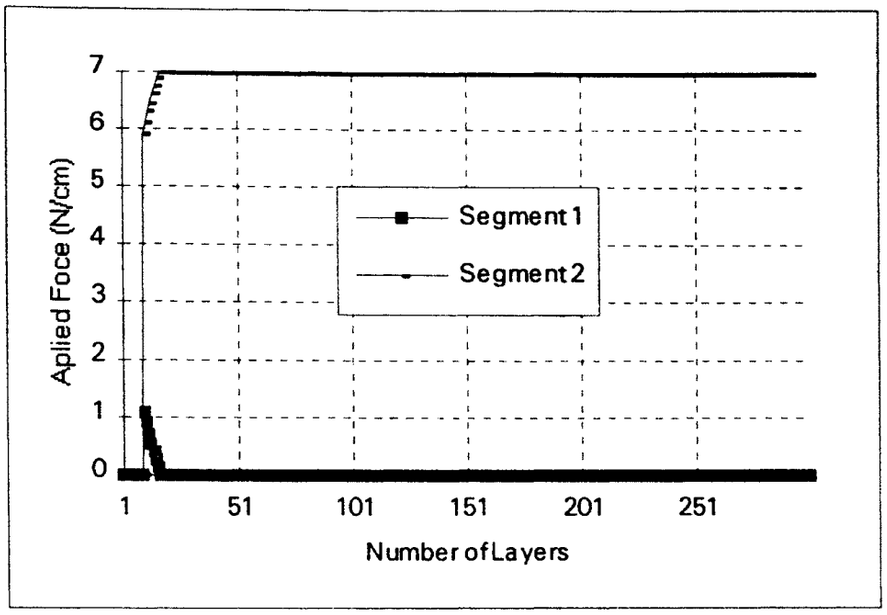

Figure 4-11. Applied Force Distribution for Set B with Nip Force 7 N/cm

Since height of the hardstreak is the radial difference between the maximum radius and the minimum radius of the wound roll segments, it is reasonable to use the height of the hardstreak as an indication of corrugations in the wound roll. The change in hardstreaks in the wound rolls with increasing of wound roll radius are shown in Figure 4-12 to Figure 4-15. By comparing the results in Figure 4-12 with figure 4-13, and Figure 4-14 with Figure 4-15, it can be concluded that greater nip force will cause lower height of hardstreak. Comparison of Figure 4-12, Figure 4-13 with Figure 4-5, and Figure 4-14, Figure 4-15 with Figure 4-5 can also confirm this statement, because the cases shown in Figure 4-4 and Figure 4-5 can be regarded as nip force equal to zero.

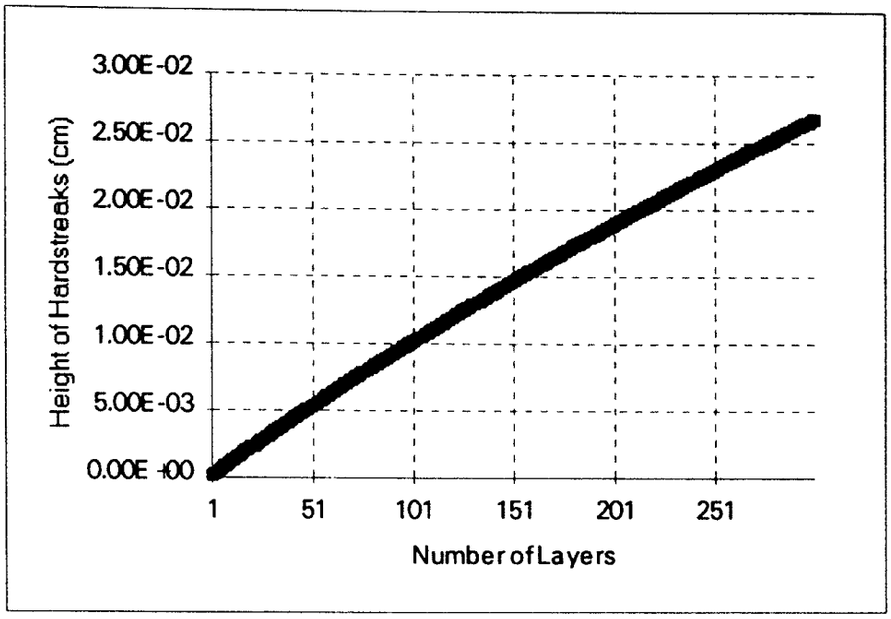

Figure 4-12. Height of Hardstreak for Set A with Nip Force 3.5 N/cm

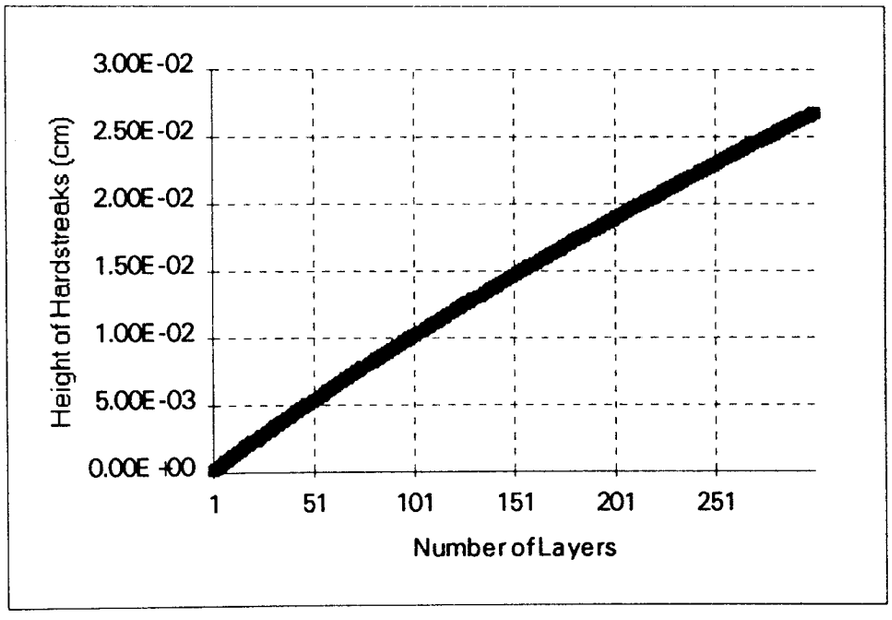

Figure 4-13. Height of Hardstreak for Set A with Nip Force 7 N/cm

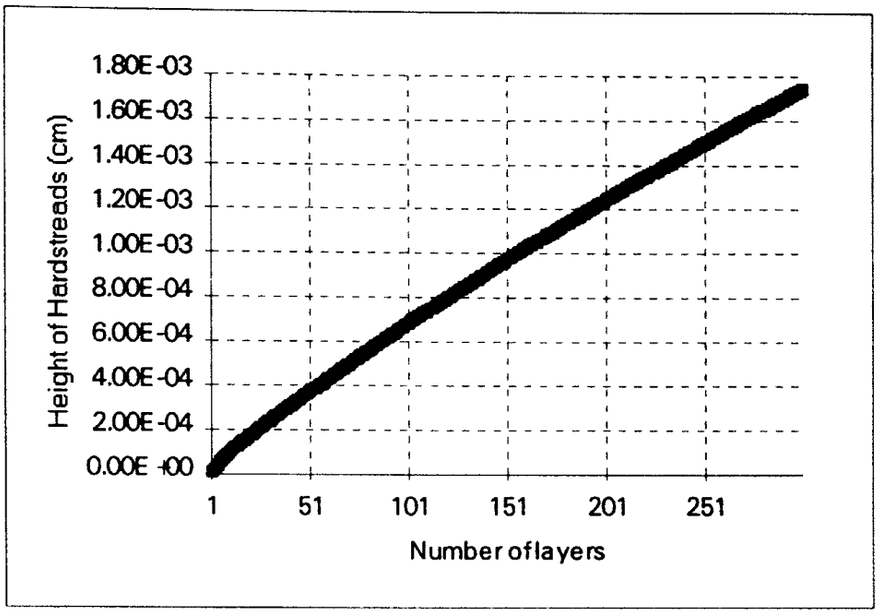

Figure 4-14. Height of Hardstreak for Set B with Nip Force 3.5 N/cm

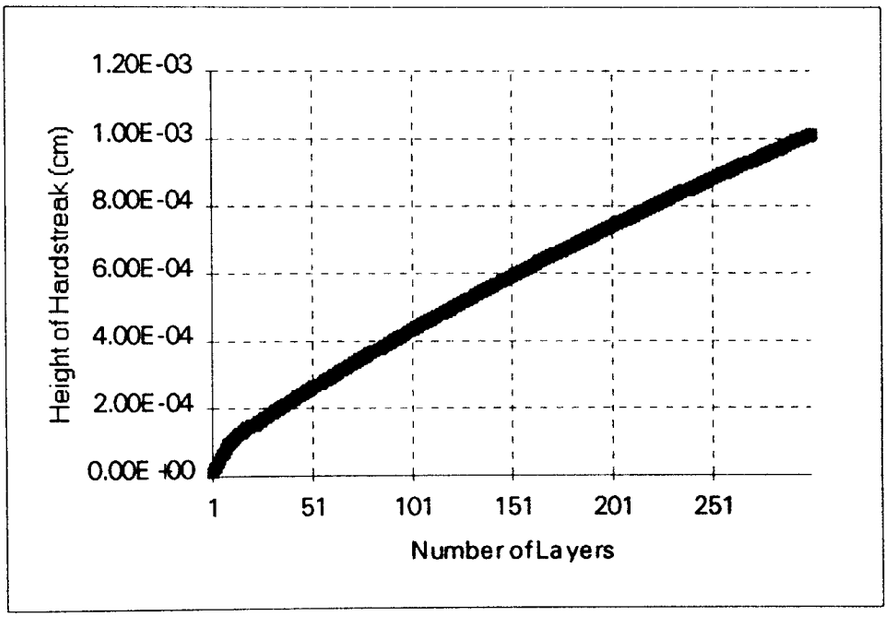

Figure 4-15. Height of Hardstreak for Set B with Nip Force 7 N/cm

In-roll pressure distributions of wound rolls are shown in Figure 4-16 to Figure 4-19. From these figures it can be seen that due to applications of the nip roller, the in-roll

pressure in the segment 1 (which contacts with the nip roller) increases as the nip force increases. The in-roll pressure in segment 2 remains unchanged because it does not make contact with the nip roller.

Effects of nip roller on the wound roll are twofold: first, application of nip roller reduces the height of hardstreak of wound roll and makes the wound roll more cylindrical; second, application of nip roller introduces more in-roll pressure and makes the distribution of in-roll pressure more uneven among these segments.

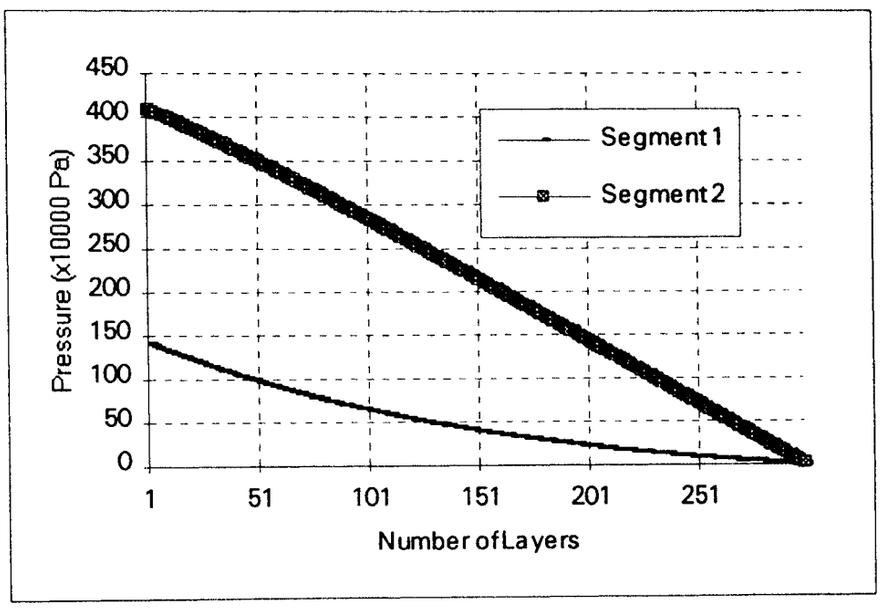

Figure 4-16. In-Roll Pressure for Set A with Nip Force 3.5 N/cm

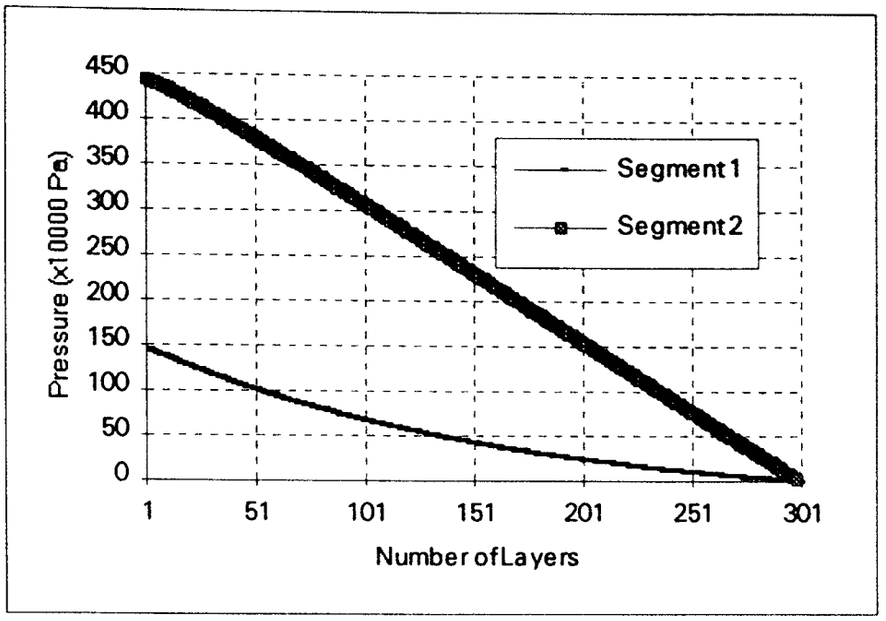

Figure 4-17. In-Roll Pressure for Set A with Nip Force 7 N/cm

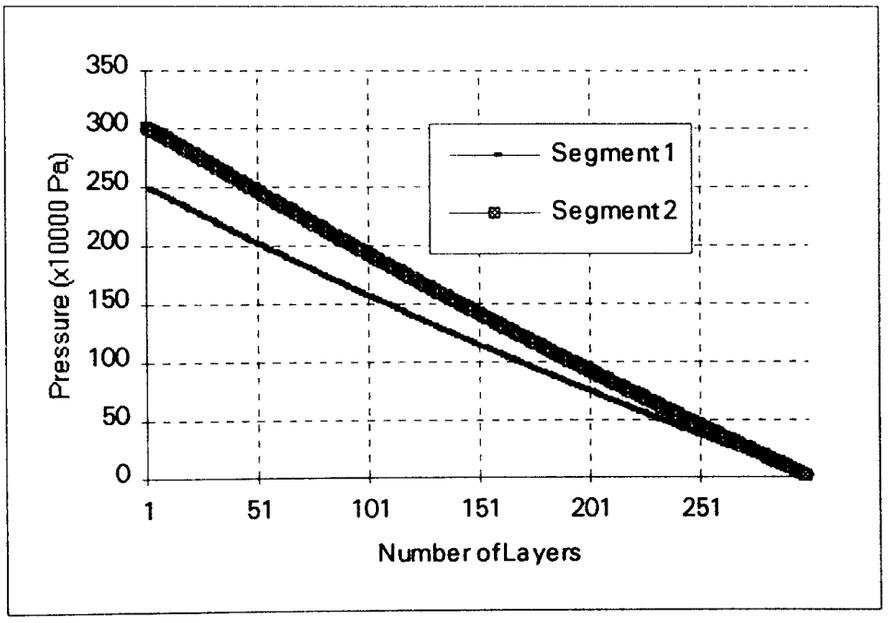

Figure 4-18. In-Roll Pressure for Set B with Nip Force 3.5 N/cm

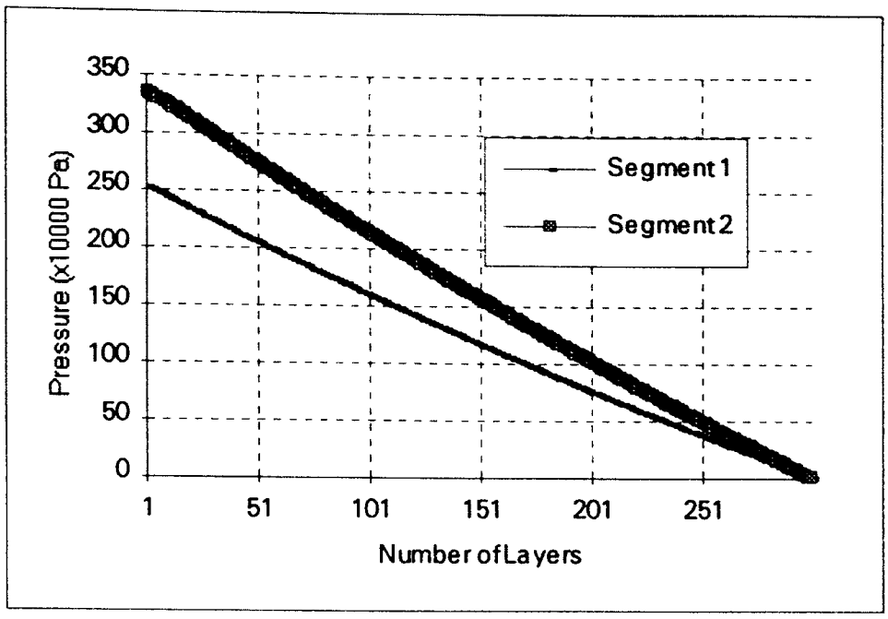

Figure 4-19. In-Roll Pressure for Set B with Nip Force 7 N/cm

In order to observe the computational results using 3-D wound roll coupled model with nip roller when much higher nip force is applied, wound roll for Set B with 550 layers are processed. The web line tension is still 7 N/cm, but the nip force is 35 N/cm, which is 5 time greater than the value previously used.

The applied force distributions are shown in Figure 4-20. From the figure it can be seen that two segments make contact with the nip roller as long as the nip roller is applied and the nip force is distributed onto the two segments.

Due to the much higher nip force applied on segments, the height of hardstreak of the wound roll does not increase as the increase of the radius, which is shown in Figure 4-21. Figure 4-21 indicates that if nip force is large enough it is possible to wind a roll with perfect cylindrical surface.

Although higher nip force helps make more round cylindrical wound roll, it also introduces much higher in-roll pressure inside the wound roll, which is shown in Figure 4-22. From Figure 4-22 it can be seen that since both segments make contact with the

nip roller, the in-roll pressure in both segments are much greater than the case in which no nip roller is applied, as shown in Figure 4-18 and Figure 4-19.

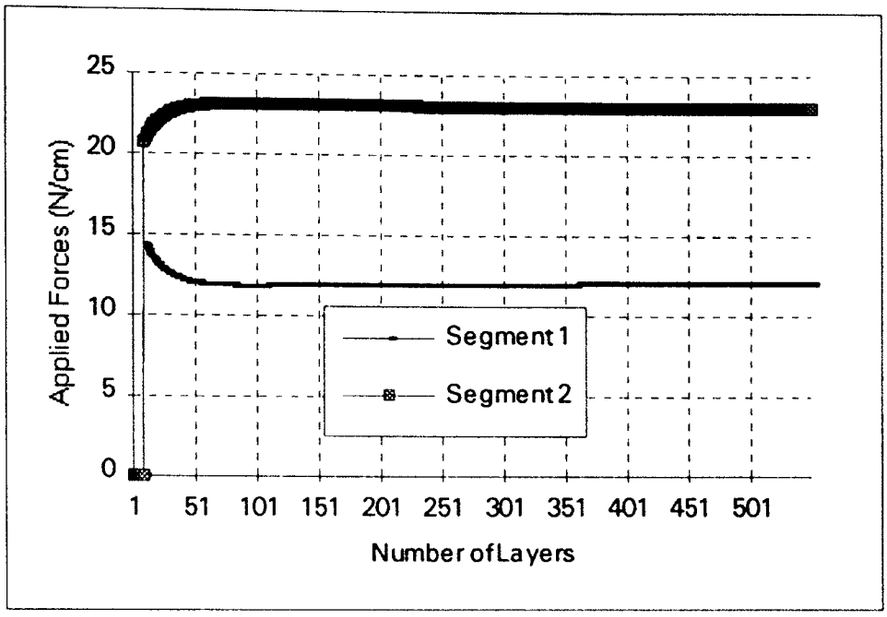

Figure 4-20. Applied Force Distribution For Set B with Nip Force 35 N/cm

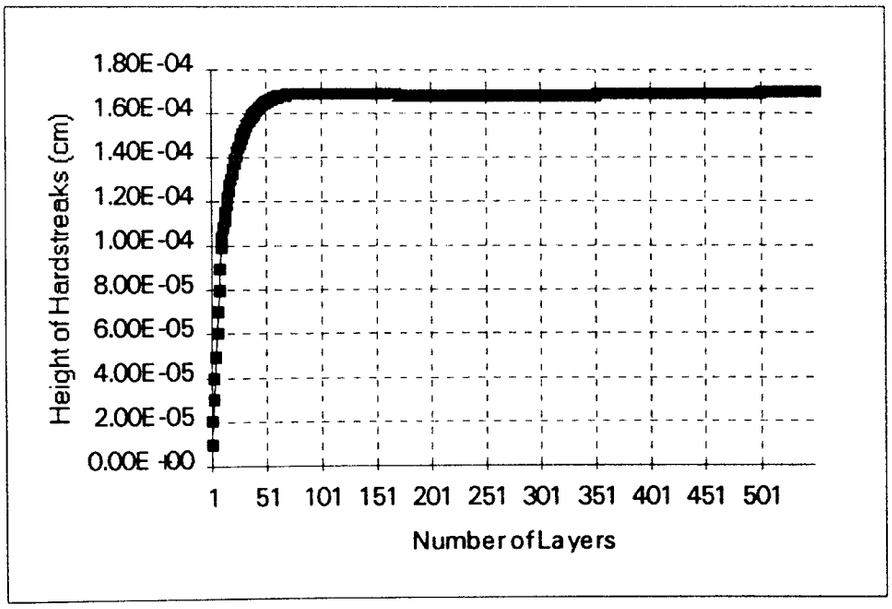

Figure 4-21. Height of Hardstreak for Set B with Nip Force 35 N/cm

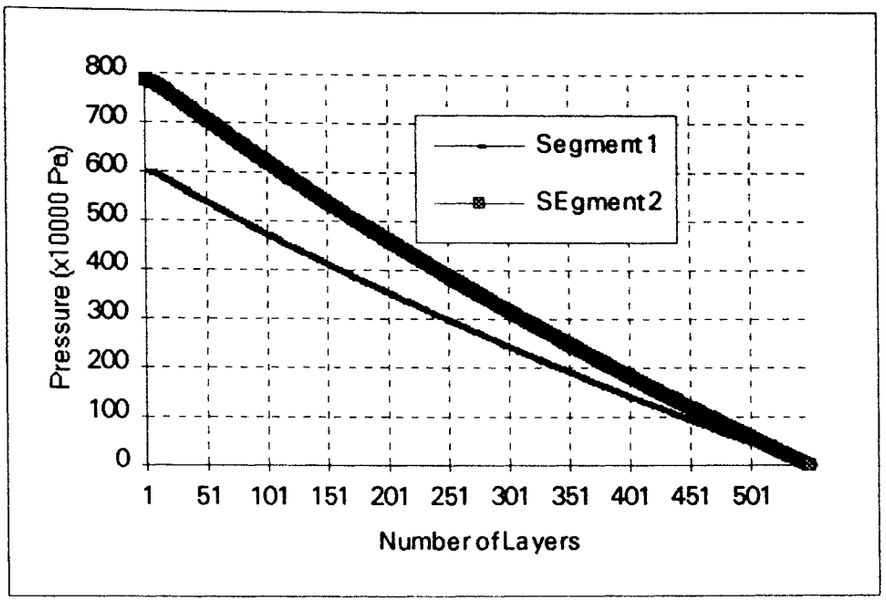

Figure. 4-22 In-Roll Pressure for Set B with Nip Force 35 N /cm

CHAPTER 5

CONCLUSION AND RECOMMENDATION FOR FUTURE WORK

5.1 Conclusions

This study has implemented the Hakiel's 3-D wound roll uncoupled model and Cole and Hakiel's 3-D wound roll coupled model. Through verifications, the source codes developed in this study have been proven valid. This study has also presented a 3-D wound roll coupled model with nip roller and implemented the source code. The model incorporating the nip is not verified.

It is concluded from this study the following points:

1). For a web with thickness variation in widthwise direction that the number of split segments which form the winding roll should be adequate in order to gain enough computational accuracy. Since the thickness variation may vary in many different forms it is impossible to generate one algorithm which would define the number of segments required to minimize error. Thus one must continue subdividing the roll into segments until solutions converge.

2). The 3-D in-roll pressure distribution is spatial and the maximum in-roll pressure is not always near the core. The maximum in-roll pressure is reduced when 3-D coupled model is used than 3-D uncoupled model is used.

3). The nip roller can reduce corrugations of the wound roll. The greater the nip load, the lower the height of a the hardstreak of the wound roll. By using a nip roller, the height of hardstreak of the winding roll can be reduced and a nearly cylindrical roll can be wound.

4). The nip roller increases the wound-on-tension and thereby the in-roll pressure will increase to very large values. This extra high in-roll pressure may cause permanent damage of wound roll such that decisions must be made to either wind non-cylindrical rolls with relatively low in-roll pressures or to wind cylindrical rolls with relatively high in-roll pressures.

5.2 Recommendations for Future Work

Since winding with nip roller is so common in web handing industry, it is very important to have a 3-D model which incorporates deformations and nip roller. This study has laid a solid foundation to develop a valid and reliable 3-D coupling model with nip roller. Therefore, future work should be conducted on this subject.

It is recommended that, the support of nip roller in the model (Figure 4-2) should be modified to allow tilt of the nip roller, since in practice almost all nip rollers can be tilted relative to the axis of winding roll.

Finally, the 3-D wound roll coupled model with a nip roller should be verified experimentally.

BIBLIOGRAPHY

1. Altmann, H. C., "Formulas for Computing the Stresses in Center-Wound Rolls." Tappi Journal, Volume 51, No. 4, pp. 176-179, April 1968.
2. Cai, Ning, "The Effect of Nip Roll Compliance upon Center and Surface Winding." M.S. Thesis, the School of Mechanical and Aerospace Engineering, Oklahoma State University, December 1992.
3. Cole, K. A. & Hakiel, Z., "A Nonlinear Wound Roll Stress Model Accounting for Widthwise Web Thickness Nonuniformities." Proceedings of the 1992 Winter Annual Meeting of the American Society of Mechanical Engineering, Symposium on Web Handling, Nov. 8-13,1992, Anaheim, California, AMD-Volume 149, pp. 13-24.
4. Good, J. K. and Fikes, M. W. R., "Predicting Internal Stresses in Center-Wound Rolls with an Undriven Nip Roller." Tappi Journal, Volume 74, No. 6, pp. 101-109, June 1991.
5. Hakiel, Z., "Nonlinear Model for Wound Roll Stresses." Tappi Journal, Volume 70, No. 5, pp. 113-117, May 1987.
6. Hakiel, Z., "On the Effect of Width Direction Thickness Variations in Wound Rolls." Proceedings of First International Conference on Web Handling, Web Handling Research Center, Stillwater, Oklahoma May 19-21, 1991.
7. Kedl, D. M., "Using of Two-Dimensional Winding Models to Predict Wound Roll Stresses that Occur due to Circumferential Steps in Core Diameter or to Cross Web Caliper Variation." Proceedings of First International Conference on Web Handling, Web Handling Research Center, Stillwater, Oklahoma May 19-21, 1991.
8. Johnson, K. L. "Contact Mechanics" Cambridge University Press, 1985.

9. Pfeiffer, J. D., "Internal Pressures in a Wound Roll of Paper." Tappi Journal, Volume 49, No. 8, pp. 342-374, August 1966.

10. Pfeiffer, J. D., "Prediction of Roll Defects from Roll Structure Formulas." Tappi Journal, Volume 62, No. 10, pp. 83-85, October 1979.

11. Pfeiffer, J. D., "Mechanics of a Rolling Nip on Paper Webs." Tappi Journal, Volume 51, No. 8, pp. 77A-85A, 1968.

12. Pfeiffer, J. D., "Nip Forces and Their Effect on Wound in Tension." Tappi Journal, Volume 60, No. 3, pp. 115-117, 1977.

13. Spitz, D. A., "Effect of Cross Direction Caliper Variation in Winding." Tappi Journal, Volume 52, No. 6, pp. 1168-1170, 1969.

14. Xu, Yaguang, "Computing Stress Distributions in Center Wound Rolls from Web Surface Characteristics." Qualifying Examinationthe School of Mechanical and Aerospace Engineering, Oklahoma State University, 1992.

VITA

Fengzhu Li

Candidate for the Degree of

Master of Science

Thesis: DEVELOPMENT OF THREE-DIMENSIONAL MODELS FOR WOUND ROLLS

Major Field: Mechanical Engineering

Biographical:

Personal Data: Born in Zibao, Shandong, P. R. China, On Nov. 15, 1962, the son of Daizhong Li and Yancai Feng.

Education: Graduated from No. 4 high school, Zibao city, Shandong, P. R. C. in 1979; receive Bachelor of Science degree in Mechanical Engineering and a Master of Science in Mechanical Engineering in Nanjing University of Aerospace and Aeronautics, Nanjing, P. R. China, in July 1983 and May 1986, respectively. Completed the requirements for the Master of Science degree with a major in Mechanical Engineering at Oklahoma state university in December 1994.

Experience: Employed by Nanjing University of Aerospace and Aeronautics and Eastern China Aero-engine Company, as an assistant professor and Engineer respectively. Employed by Department of Aerospace and Mechanical Engineering, Oklahoma State University as a research assistant, 1992 to present.